

Lepton Flavor Violation of Z Gauge Boson Decays in Supersymmetric Type-III Seesaw Model

Vael Hajahmad^{1, 2*} and Murhaf AlSayed Ali³

^{1*}Physics Department, Erzincan University, Turkey.

²Physics Department, Al-Furat University, Syria.

³Physics Department, Idlib University, Syria.

*Corresponding author(s). E-mail(s): whahmad@erzincan.edu.tr;
Contributing authors: morhaf.alsayed.ali@idlib-university.com;

Abstract

In this study, we investigate the lepton flavor violation (LFV) of Z gauge boson decaying into two different flavor charged leptons $Z \rightarrow l_i l_j$ ($Z \rightarrow \tau\mu$, $Z \rightarrow \tau e$ and $Z \rightarrow \mu e$). This work is performed in the framework of the constrained minimal supersymmetric standard model (CMSSM) which is extended by the type-III seesaw mechanism. By considering constraints from the current experimental bounds on neutrino and supersymmetric particle masses, we calculate the branching ratios of the LFV of Z boson decays. The numerical results are found to be 1.30×10^{-9} for both the $\tau\mu$ and τe decay channels and 6.40×10^{-10} for the μe channel. After applying the constraints from the experimental bounds on the radiative two body decays $l_i \rightarrow l_j \gamma$, the branching ratios of the LFV of Z boson decays get an additional suppression of 10^{-3} for the $\tau\mu$ and τe decay channels and 10^{-8} for the μe channel. The prediction of the branching ratios is found to be several orders of magnitude below the current experimental bounds for both scenarios. Thus the LFV of Z boson decays could be observed with low likelihood in the future collider experiments.

Keywords: Lepton Flavor Violation, MSSM Model, Type-III Seesaw Model

1 Introduction

The lepton flavor is conserved in the standard model (SM). The observation of neutrino oscillations enable the lepton flavor violation to occur [1]. The SM of elementary

particles is a very successful model for explaining of many physical phenomena, which contain a wide range of energy scales that can be covered by the current experiments. However, the SM cannot be considered a complete theory because of its inability to give the neutrinos their mass [2]. One of the unresolved issues in modern physics is origin of the neutrino mass, which has been discovered by the neutrino oscillation experiments [3–6]. The mass upper limit in the Karlsruhe tritium neutrino experiment (KATRIN) is estimated to be 1.1 eV (90% CL) in 2021 [7], later on in 2022 it is estimated to be 0.8 eV (90% CL) [8].

Neutrinos are massless in the SM, but the observation of neutrino oscillations indicate that neutrinos have tiny masses. This means that the SM needs to be extended by new mechanisms [9, 10]. The most popular ideas for generating the neutrino masses are the so-called seesaw mechanism, which provides a minimal framework to explain origin of the neutrino masses [9, 11]. The seesaw mechanism can be classified into three primary types: Type-I, type-II and type-III. The type-I and type-III seesaw models introduce three additional singlet(triplet) fermions [12–18], whereas the type-II seesaw model introduces an additional triplet scalar [16, 19–24].

The study of rare decays like the lepton flavor violation (LFV) is crucial in exploring new physics beyond the standard model (BSM). The LFV decays are of interest because they are suppressed in the SM, so their detection would serve as a clear indication of new physics. The quest to detect such rare decays is ongoing, with investigations being conducted in a variety of processes involving leptons, Z boson, Higgs, Z' and various hadrons [25, 26].

However, there are many new physical models (BSM) where the branching ratios (BRs) of the LFV decays can be increased to fall within the detectable range of the current experiments. These models are: grand unified, two Higgs doublets, supersymmetric and left-right symmetry models. It is demonstrated that the predicted branching ratios in these various extensions of the SM could potentially be detected by the current or future experiments [27].

The supersymmetry (SUSY) is a well-motivated solution to the hierarchy problem that also offers an elegant one to the non-baryonic dark matter (DM) problem of the universe. If large hadron collider (LHC) indeed finds signatures of SUSY, it is then extremely appealing to consider the embedding of seesaw mechanism into the supersymmetric framework the so-called SUSY seesaw models. These models perhaps lead to the possibility of having the lepton flavor violation in Z boson, Higgs, tau and muon decays [28].

Based on the fact that the SM predictions for the LFV of Z boson decays ($Z \rightarrow \tau\mu$, $Z \rightarrow \tau e$ and $Z \rightarrow \mu e$) are suppressed by the neutrino masses. This makes them undetectable by the current experiments at the LHC (ATLAS and CMS). By considering the neutrino masses, the SM predictions for the branching ratios of these decays are estimated to be between 10^{-50} and 10^{-40} . Therefore, any experimental detection of the Z boson LFV decays would indicate the presence of new physics [29]. According to the recent results of the ATLAS experiment [30, 31] and to the expected sensitivity of the future colliders (FCC-ee/CEPC) [32, 33], the experimental upper limits of BRs of the Z boson decay channels ($Z \rightarrow \tau e$, $Z \rightarrow \tau\mu$ and $Z \rightarrow \mu e$) are shown in table 1.

Table 1: Experimental upper limits and expected sensitivity of the branching ratios of the lepton flavor violating Z boson decays.

Collider	LHC (95%CL)	FCC-ee/CEPC
$BR(Z \rightarrow \tau e)$	7×10^{-6} [30]	10^{-9} [32, 33]
$BR(Z \rightarrow \tau \mu)$	7.20×10^{-6} [30]	10^{-9} [32, 33]
$BR(Z \rightarrow \mu e)$	2.62×10^{-7} [31]	$10^{-8} - 10^{-10}$ [32, 33]

We focus in this study on the Z boson decays into two different charged lepton flavors $Z \rightarrow l_i l_j$ where $l_i, l_j = e, \mu$ and τ . Thus, the work is implemented in the framework of the constrained scenario of the minimal supersymmetric standard model (CMSSM), which is extended by the type-III seesaw model (adding a supersymmetric fermionic triplet field).

In the SUSY seesaw model, the large flavor mixings of sleptons induce LFV interactions $l_i \bar{l}_j V$ ($V = \gamma, Z$). As a result of this, there exists a correlation between the branching ratios of $Z \rightarrow l_i l_j$ and the radiative two body decays $l_i \rightarrow l_j \gamma$ [34–36]. The experimental upper limits on both masses of SUSY particles and radiative two body decays $l_i \rightarrow l_j \gamma$ will be considered to constraint the model parameters, then to evaluate the branching ratios of $Z \rightarrow l_i l_j$ with(without) imposing constraints on the $l_i \rightarrow l_j \gamma$ decays.

2 MSSM-Seesaw Type-III model

In the case of type-II and type-III seesaw models, if the MSSM model is extended by just the superfields which are responsible for the neutrino masses and mixings, the nice feature of gauge coupling unification would be destroyed because it belongs to incomplete SU(5) representations. This problem can be solved by embedding new states in complete SU(5) representations. For instance, 15-plets in the case of the type-II seesaw model while 24-plets in the case of the type-III seesaw model [28, 37, 38].

In the type-III seesaw model, the MSSM spectrum of particles is extended by adding a fermionic triplet superfield with zero hypercharge belonging to the adjoint representation of $SU(2)_L$ [37]. It is not sufficient to add one generation of 24-plets to explain all neutrino data if we suppose SU(5) invariant boundary conditions at the grand unified theory (GUT) scale. Therefore, the splitting of the induced mass between different neutrino generations will not be sufficiently large. Thus, we will add three generations of 24-plets. The 24-plets decompose under the standard model gauge group $SU(3)_C \times SU(2)_L \times U(1)_Y$ as follows [28, 37, 39, 40]:

$$\begin{aligned}
 24_M &= \hat{G}_M + \hat{W}_M + \hat{B}_M + \hat{X}_M + \hat{\bar{X}}_M \\
 &= (8, 1, 0) + (1, 3, 0) + (1, 1, 0) + (\bar{3}, 2, \frac{5}{6}) + (3, 2, -\frac{5}{6})
 \end{aligned}$$

The two fermionic components, $\hat{B}_M(1, 1, 0)$ and $\hat{W}_M(1, 3, 0)$, possess exactly the same quantum numbers as a singlet right-handed neutrino ν_R and a fermionic triplet respectively. Thus, if these components are embedded into the SU(5) framework, the type-III

seesaw model realization will generally produce a mixture of both type-III and type-I mechanisms [28, 37, 39].

Table 2 and table 3 show quantum numbers of the gauge symmetry group for the chiral superfields and the vector (gauge bosons) superfields in the MSSM-Seesaw type-III model.

Table 2: The chiral superfields and their quantum numbers in the MSSM-Seesaw type-III model. Where \hat{Q} , \hat{L} , \hat{H}_d and \hat{H}_u are superfields of left quarks, left leptons, down-Higgs and up-Higgs. While \hat{d} , \hat{u} and \hat{l} are superfields of right down-quarks, right up-quarks and right leptons.

SF	Spin 0	Spin $\frac{1}{2}$	Generations	$(U(1) \otimes SU(2) \otimes SU(3))$
\hat{Q}	\tilde{q}	q	3	$(\frac{1}{6}, 2, 3)$
\hat{L}	\tilde{L}	L	3	$(-\frac{1}{2}, 2, 1)$
\hat{H}_d	H_d	\tilde{H}_d	1	$(-\frac{1}{2}, 2, 1)$
\hat{H}_u	H_u	\tilde{H}_u	1	$(\frac{1}{2}, 2, 1)$
\hat{d}	\tilde{d}_R^*	d_R^*	3	$(\frac{1}{3}, 1, \bar{3})$
\hat{u}	\tilde{u}_R^*	u_R^*	3	$(-\frac{2}{3}, 1, \bar{3})$
\hat{l}	\tilde{l}_R^*	l_R^*	3	$(1, 1, 1)$
\hat{W}_M	\tilde{W}_M	W_M	3	$(0, 3, 1)$
\hat{G}_M	\tilde{G}_M	G_M	3	$(0, 1, 8)$
\hat{B}_M	\tilde{B}_M	B_M	3	$(0, 1, 1)$
\hat{X}_M	\tilde{X}_M	X_M	3	$(\frac{5}{3}, 2, \bar{3})$
$\hat{\tilde{X}}_M$	$\tilde{\tilde{X}}_M$	\tilde{X}_M	3	$(-\frac{5}{3}, 2, 3)$

Table 3: The vector (gauge bosons) superfields in the MSSM-Seesaw Type-III model and their quantum numbers.

SF	Spin $\frac{1}{2}$	Spin 1	$(U(1) \otimes SU(2) \otimes SU(3))$
\hat{G}^a	\tilde{G}^a	G^a	$(0, 1, 8)$
\hat{W}^b	$\tilde{W}^0, \tilde{W}^\pm$	W^0, W^\pm	$(0, 3, 1)$
\hat{B}	\tilde{B}	B	$(0, 1, 1)$

The breaking phase of SU(5) leads to that the superpotential is below the GUT scale [37, 39–41], the superpotential is defined as follows:

$$W = W_{MSSM} + W_{SeesawIII} \quad (1)$$

Where W_{MSSM} represents the superpotential for the minimal supersymmetric standard model (MSSM). $W_{SeesawIII}$ represents the superpotential for the SUSY type-III seesaw model. W_{MSSM} and $W_{SeesawIII}$ can be written as follows:

$$W_{MSSM} = Y_u \hat{u} \hat{Q} \hat{H}_u - Y_d \hat{d} \hat{Q} \hat{H}_d - Y_l \hat{l} \hat{L} \hat{H}_d + \mu \hat{H}_u \hat{H}_d \quad (2)$$

$$\begin{aligned}
W_{seesaw-III} = & \hat{H}_u (\hat{W}_M Y_W - \sqrt{\frac{3}{10}} \hat{B}_M Y_B) \hat{L} + \hat{H}_u \hat{X}_M Y_X \hat{d}_R \\
& + \frac{1}{2} \hat{B}_M M_B \hat{B}_M + \frac{1}{2} \hat{G}_M M_G \hat{G}_M + \frac{1}{2} \hat{W}_M M_W \hat{W}_M + \hat{X}_M M_X \hat{X}_M \quad (3)
\end{aligned}$$

At heavy fields scale (seesaw scale), below the M_{GUT} scale, the Weinberg operator is generated as follows [28]:

$$\frac{1}{2} k_\nu \hat{L} \hat{L} \hat{H}_u \hat{H}_u \quad (4)$$

Where $k_\nu = \frac{3}{10} Y_B^t M_B^{-1} Y_B + \frac{1}{2} Y_W^t M_W^{-1} Y_W$

In the MSSM-Seesaw type-III model, terms of the soft supersymmetric breaking (SUSY breaking) are given as in the following equation [39, 41]:

$$\begin{aligned}
-\mathcal{L}_{soft} = & \mathcal{L}_{soft-MSSM} + \frac{\sqrt{3}}{\sqrt{10}} A_B Y_B H_u \tilde{B}_M \tilde{L} + A_W Y_W H_u \tilde{W}_M \tilde{L} + A_X Y_X H_u \tilde{X}_M \tilde{d}^c \\
& + \frac{1}{2} B_W M_W \tilde{W}_M \tilde{W}_M + \frac{1}{2} B_G M_G \tilde{G}_M \tilde{G}_M + \frac{1}{2} B_B M_B \tilde{B}_M \tilde{B}_M \\
& + B_X M_X \tilde{W}_M \tilde{X}_M + h.c. + m_B^2 \tilde{B}_M^\dagger \tilde{B}_M + m_W^2 \tilde{W}_M^\dagger \tilde{W}_M + m_G^2 \tilde{G}_M^\dagger \tilde{G}_M \\
& + m_X^2 \tilde{X}_M^\dagger \tilde{X}_M + m_{\tilde{X}}^2 \tilde{X}_M^\dagger \tilde{X}_M \quad (5)
\end{aligned}$$

Where m_W^2 , m_G^2 , m_X^2 and $m_{\tilde{X}}^2$ represent the square of soft mass terms for the triplet fermion \tilde{W}_M , singlet fermions (\tilde{G}_M, \tilde{B}_M) and fermionic doublets (\tilde{X}_M, \tilde{X}_M) respectively. A_B, A_W, A_X are tri-linear couplings. B_W, B_G and B_B are bi-linear couplings [41]. $\mathcal{L}_{soft, MSSM}$ for the sleptons and the gauge sector are written as follows:

$$\begin{aligned}
-\mathcal{L}_{soft, Slepton} = & \sum_{i,j=gen} (m_{\tilde{L}}^2)_{ij} \tilde{L}_i^* \tilde{L}_j + (m_{\tilde{l}_R}^2)_{ij} \tilde{l}_{Ri}^* \tilde{l}_{Rj} + (m_{\tilde{\nu}_L}^2)_{ij} \tilde{\nu}_{Li}^* \tilde{\nu}_{Lj} \\
& + \sum_{i,j=gen} A_{ij}^l Y_{ij}^l \tilde{l}_{Ri}^* \tilde{L}_j H_d + h.c. \quad (6)
\end{aligned}$$

$$-\mathcal{L}_{soft, gaugino} = \frac{1}{2} M_3 \tilde{G} \tilde{G} + \frac{1}{2} M_2 \tilde{W} \tilde{W} + \frac{1}{2} M_1 \tilde{B} \tilde{B} + h.c. \quad (7)$$

Where M_1, M_2 and M_3 are three gaugino mass parameters for the bino, wino and gluino terms respectively [42, 43]. $m_{\tilde{L}}^2$ and $m_{\tilde{l}_R}^2$ represent the square of mass terms for the supersymmetric leptons. i and j indicate to the generation number. $T_{ij}^l = A_{ij}^l Y_{ij}^l$ where A_{ij}^l represents terms of the tri-linear coupling and h.c. is the hermitian conjugate. Terms for squarks and Higgs are determined in the same way as in the MSSM [42].

In the MSSM-Seesaw type-III model, after the electroweak symmetry breaking (EWSB), the mass matrices of neutralinos, sleptons and sneutrinos (taking in to account that sneutrinos are disparted into CP-odd sneutrinos and CP-even sneutrinos) can be introduced as follows:

$$\tilde{\nu}_L = \frac{1}{\sqrt{2}}[\phi_L + i\sigma_L] \quad (8)$$

Thus, the mass matrix for CP-odd sneutrinos $m_{\nu I}^2$ is written as:

$$\begin{aligned} m_{\nu I}^2 = m_{\sigma_L \sigma_L} = & + \frac{1}{8} (g_1^2 + g_2^2) (-v_u^2 + v_d^2) + \Re(m_L^2) \\ & + \frac{1}{16} v_u^4 \left[\Re(\kappa_\nu \kappa_\nu^*) + \Re(\kappa_\nu \kappa_\nu^\dagger) + \Re(\kappa_\nu^t \kappa_\nu^*) + \Re(\kappa_\nu^t \kappa_\nu^\dagger) \right] \\ & + \frac{1}{4} v_u^2 \Re(Y_W^t Y_W^*) + \frac{3}{20} v_u^2 \Re(Y_B^t Y_B^*) \\ & + \frac{1}{8} v_u v_d \left[2\mu (\kappa_{\nu, o_1}^* + \kappa_{\nu, p_1}^*) + \mu^* (\kappa_\nu + \kappa_\nu^t + \kappa_{\nu, o_1} + \kappa_{\nu, p_1}) \right] \end{aligned} \quad (9)$$

Where g_1 and g_2 are gauge coupling constants of the electromagnetic $U(1)_Y$ and the weak $SU(2)_L$ interactions, v_u and v_d are the vacuum expectation values of H_u and H_d respectively. The indices o_1 and p_1 refer to the first generation. The mass matrix for CP-odd sneutrinos $m_{\nu I}^2$ is diagonalized by Z^i :

$$Z^i m_{\nu I}^2 Z^{i, \dagger} = \text{diag}(m_{\tilde{\nu}_1^I}^2, m_{\tilde{\nu}_2^I}^2, m_{\tilde{\nu}_3^I}^2) \quad (10)$$

The mass matrix for CP-even sneutrinos $m_{\nu R}^2$ is written as:

$$\begin{aligned} m_{\nu R}^2 = m_{\phi_L \phi_L} = & \frac{1}{8} (g_1^2 + g_2^2) (-v_u^2 + v_d^2) + \Re(m_L^2) \\ & + \frac{1}{16} v_u^4 \left[\Re(\kappa_\nu \kappa_\nu^*) + \Re(\kappa_\nu \kappa_\nu^\dagger) + \Re(\kappa_\nu^t \kappa_\nu^*) + \Re(\kappa_\nu^t \kappa_\nu^\dagger) \right] \\ & + \frac{1}{4} v_u^2 \Re(Y_W^t Y_W^*) + \frac{3}{20} v_u^2 \Re(Y_B^t Y_B^*) \\ & - \frac{1}{8} v_u v_d \left[2\mu (\kappa_{\nu, o_1}^* + \kappa_{\nu, p_1}^*) + \mu^* (\kappa_\nu + \kappa_\nu^t + \kappa_{\nu, o_1} + \kappa_{\nu, p_1}) \right] \end{aligned} \quad (11)$$

This matrix is diagonalized by Z^R :

$$Z^R m_{\nu R}^2 Z^{R, \dagger} = \text{diag}(m_{\tilde{\nu}_1^R}^2, m_{\tilde{\nu}_2^R}^2, m_{\tilde{\nu}_3^R}^2) \quad (12)$$

Where the terms in the second, third and fourth lines of equations (9, 11) are newly introduced by the MSSM-Seesaw type-III model. The slepton mass squared matrix can be expressed as:

$$M_l^2 = \begin{pmatrix} M_{LL} & M_{LR} \\ M_{RL} & M_{RR} \end{pmatrix} \quad (13)$$

$$M_{LL} = \frac{1}{2}v_d^2 Y_l^\dagger Y_l + \frac{1}{8}(-g_2^2 + g_1^2)(-v_u^2 + v_d^2) + m_{\tilde{L}}^2 \quad (14)$$

$$M_{RR} = \frac{1}{2}v_d^2 Y_l Y_l^\dagger + \frac{1}{4}g_1^2(-v_d^2 + v_u^2) + m_{\tilde{t}_R}^2 \quad (15)$$

$$M_{LR} = \frac{1}{\sqrt{2}}(v_d T_l^\dagger - v_u \mu Y_l^\dagger) \quad (16)$$

$$M_{RL} = M_{LR}^\dagger = \frac{1}{\sqrt{2}}(v_d T_l - v_u Y_l \mu^*) \quad (17)$$

Where μ is the Higgsino mass parameter. This matrix is diagonalized by Z^E :

$$Z^E M_{\tilde{l}}^2 Z^{E,\dagger} = \text{diag}(m_{\tilde{l}_1}^2, \dots, m_{\tilde{l}_6}^2) \quad (18)$$

The lepton flavor violation sources are off-diagonal entries of 3×3 soft SUSY breaking matrices $m_{\tilde{L}}^2, m_{\tilde{t}_R}^2$. The neutralino mass matrix can be expressed as:

$$m_{\tilde{\chi}^0} = \begin{pmatrix} M_1 & 0 & -\frac{1}{2}g_1 v_d & \frac{1}{2}g_1 v_u \\ 0 & M_2 & \frac{1}{2}g_2 v_d & -\frac{1}{2}g_2 v_u \\ -\frac{1}{2}g_1 v_d & \frac{1}{2}g_2 v_d & 0 & -\mu \\ \frac{1}{2}g_1 v_u & -\frac{1}{2}g_2 v_u & -\mu & 0 \end{pmatrix} \quad (19)$$

This matrix is diagonalized by N :

$$N^* m_{\tilde{\chi}^0} N^\dagger = \text{diag}(m_{\tilde{\chi}_1^0}, m_{\tilde{\chi}_2^0}, m_{\tilde{\chi}_3^0}, m_{\tilde{\chi}_4^0}) \quad (20)$$

The chargino mass matrix is given by:

$$m_{\tilde{\chi}^\pm} = \begin{pmatrix} M_2 & \frac{1}{\sqrt{2}}g_2 v_u \\ \frac{1}{\sqrt{2}}g_2 v_d & \mu \end{pmatrix} \quad (21)$$

This matrix is diagonalized by U and V

$$U^* m_{\tilde{\chi}^\pm} V^\dagger = \text{diag}(m_{\tilde{\chi}_1^\pm}, m_{\tilde{\chi}_2^\pm}) \quad (22)$$

The flavor mixing of charged sleptons and CP-odd (CP-even) sneutrinos induces the flavor-changing neutral-current couplings (FCNC) $\tilde{\chi}^0 \tilde{l} \tilde{l}$ and $Z \tilde{l} \tilde{l}$, while the flavor mixing of left-handed sneutrinos induces flavor-changing charged-current couplings $\tilde{\chi}^+ l \tilde{\nu}$. These flavor-changing couplings will contribute to the LFV of Z-decays ($Z \rightarrow l_i l_j$) [34, 44], as shown in Fig.1.

The mass matrix of the light neutrino is yielded by the EWSB as in the following equation [28, 37, 39–41]:

$$m_\nu = \frac{-v_u^2}{2} \left[\frac{3}{10} Y_B^t M_B^{-1} Y_B + \frac{1}{2} Y_W^t M_W^{-1} Y_W \right] \quad (23)$$

The type-III formula has two contributions as shown in equation (23), one arising from the $SU(2)_L$ singlet ($\propto Y_B$) and the other arising from the $SU(2)_L$ triplet ($\propto Y_W$) part of the superpotential respectively. Thus, in this situation, the calculation of Yukawa couplings is more complicated. It can be simplified by the following approximation: As we suppose universal masses and couplings at the GUT scale, we find that the seesaw scale is still quite high. Therefore, we can suppose that $Y_B \simeq Y_W$ and $M_B \simeq M_W$ at the seesaw scale. So, we can write the equation (23) as follows [28, 37, 39–41]:

$$m_\nu = -\frac{2}{5}v_u^2 Y_W^t M_W^{-1} Y_W \quad (24)$$

The light neutrino mass matrix is diagonalized by the lepton mixing matrix:

$$U^{V,*} m_\nu U^{V,\dagger} = m_\nu^{dia} = \text{diag}(m_{\nu_1}, m_{\nu_2}, m_{\nu_3}) \quad (25)$$

The equation (24) depends on a high energy scale ($M_W \sim 10^{14}$ GeV for $Y_W \sim 1$) [40]. In order to calculate the neutrino mass at low energy, we need to know the values of both M_W and Y_W as input parameters at $M_{GUT} \sim 10^{16}$ GeV. Furthermore, it is obvious from equation (24) that the Y_W matrix is similar to the Y_ν one, because both matrices are diagonalized by the U^V matrix (lepton mixing matrix). Thus, the structure of Y_W matrix can be like the one of Y_ν matrix ($Y_W=Y_\nu$) [1, 28, 37, 39].

In the general MSSM model, in the slepton mass matrices the LFV off-diagonal entries involve additional free parameters arising from the SUSY breaking mechanism. We should suppose some particular conditions for the supersymmetry breaking to relate LFV in the slepton sector with LFV encoded in the SUSY type-III seesaw model [1, 28]. We will consider the CMSSM model at the GUT scale. Hence, the supposed global conditions are as follows: The soft gaugino masses combine to a common value of $M_1 = M_2 = M_3 = m_{1/2}$. The square of the supersymmetry breaking masses of the supersymmetric fermions combine to a common value of $m_{l_R}^2 = m_L^2 = m_W^2 = m_B^2 = m_X^2 = m_{\bar{X}}^2 = m_G^2 = m_0^2 I$. Terms of the trilinear couplings combine to a common value of $A_l = A_W = A_B = A_X = A_0$ where $T_{ij}^l = A_{ij}^l Y_{ij}^l$, $T_W = A_W Y_W$, $T_B = A_B Y_B$ and $T_X = A_X Y_X$. Furthermore, m_0 is a universal scalar mass, A_0 is a universal mass parameter for the trilinear terms and $m_{1/2}$ is the common gaugino mass [28, 40, 41].

We suppose a scenario for both the tri-linear and the mass terms of W, B and X as $T_W = T_B = T_X$ where $Y_W = Y_B = Y_X$ and for the mass terms $M_W = M_B = M_G = M_X$. Furthermore, the MSSM-Seesaw type-III model contains new bilinear soft breaking parameters in the superpotential (B_W, B_B and B_G). While at the scale of seesaw, the bilinear soft breaking parameters have a tiny effect in the calculation of the thresholds and do not have any influence on the renormalization group equations (RGEs) of the other parameters, so we can safely neglect them [37].

The contribution to mixing of the supersymmetric leptons at one loop is represented by the renormalization group equations (RGEs) [28, 39] where the lepton flavor violation occurs in the left-handed sleptons sector:

$$\begin{aligned}
\Delta m_L^2 &= -\frac{9}{5} \frac{1}{8 \pi^2} m_0^2 \left\{ 3 + \frac{A_0^2}{m_0^2} \right\} Y_W^\dagger Y_W \log \left(\frac{M_{GUT}}{M_W} \right) \\
\Delta T_l^2 &= \frac{-9}{5} \frac{3}{16 \pi^2} A_0 Y_l Y_W^\dagger Y_W \log \left(\frac{M_{GUT}}{M_W} \right) \\
\Delta m_{l_R}^2 &= 0
\end{aligned} \tag{26}$$

The presence of Yukawa coupling matrix Y_W in equation (26) induces LFV in the supersymmetric left-handed lepton matrix. In addition, the non-trivial flavor structure of Y_W induces off-diagonal entries in the slepton squared mass matrices. We also notice that the terms of the right-handed supersymmetric leptons do not receive any contribution to the log-decimal approximation. Furthermore, we notice that the trilinear coupling terms are suppressed by the charged lepton masses [28, 39, 43].

We need to define the structure of a the Yukawa coupling matrix Y_W taking into account the contribution of Y_W in the LFV as in equation (26). We also consider the real values of the Y_W matrix to avoid the possible constraints from the moments of the lepton electric dipole ($Y_W^\dagger Y_W = Y_W^t Y_W$). It is effectively useful and constructive to consider a geometrical interpretation for the Yukawa coupling matrix where its elements are interpreted in the flavor space as components of three generic neutrino vectors (\mathbf{n}_μ , \mathbf{n}_e and \mathbf{n}_τ). We can write the Yukawa coupling matrix in the flavor space as follows [45, 46]:

$$Y_W = \begin{pmatrix} y_{W11} & y_{W12} & y_{W13} \\ y_{W21} & y_{W22} & y_{W23} \\ y_{W31} & y_{W32} & y_{W33} \end{pmatrix} \equiv f(\mathbf{n}_e \ \mathbf{n}_\mu \ \mathbf{n}_\tau) \tag{27}$$

Where f is the strength of the neutrino Yukawa coupling. \mathbf{n}_μ , \mathbf{n}_e and \mathbf{n}_τ are components of the three generic neutrino vectors in the flavor space. The term $Y_W^\dagger Y_W$ in RGEs equations (26) is related to LFV processes. We can write the term $Y_W^\dagger Y_W$ as follows:

$$Y_W^\dagger Y_W = f \begin{pmatrix} \mathbf{n}_e \\ \mathbf{n}_\mu \\ \mathbf{n}_\tau \end{pmatrix} f(\mathbf{n}_e \ \mathbf{n}_\mu \ \mathbf{n}_\tau) = f^2 \begin{pmatrix} |n_e|^2 & \mathbf{n}_e \cdot \mathbf{n}_\mu & \mathbf{n}_e \cdot \mathbf{n}_\tau \\ \mathbf{n}_\mu \cdot \mathbf{n}_e & |n_\mu|^2 & \mathbf{n}_\mu \cdot \mathbf{n}_\tau \\ \mathbf{n}_\tau \cdot \mathbf{n}_e & \mathbf{n}_\tau \cdot \mathbf{n}_\mu & |n_\tau|^2 \end{pmatrix} \tag{28}$$

Where $\mathbf{n}_i \cdot \mathbf{n}_j = |n_i| \cdot |n_j| \cdot C_{ij}$. $C_{ij} \equiv \cos \theta_{ij}$ is the cosine of three neutrino flavor angles $C_{\tau\mu}$, $C_{\mu e}$ and $C_{\tau e}$. The angle names are induced by the certainty that the cosine of the angle θ_{ij} controls the transitions of LFV in the $l_i - l_j$ sector. Consequently, the nine input parameters that determine the Y_W matrix can be considered as: Three modulus of the three neutrino vectors ($|n_e|, |n_\mu|, |n_\tau|$), three relative flavor angles between these vectors ($\theta_{\mu e}, \theta_{\tau e}, \theta_{\tau\mu}$) and three additional angles ($\theta_1, \theta_2, \theta_3$) which determine the global rotation \mathcal{O} of the three neutrino vectors without changing their relative angles [45, 46]. The Y_W matrix values are real, so the Y_W matrix can be written as a product of two matrices:

$$Y_W = \mathcal{O} A \tag{29}$$

Where \mathcal{O} is the orthogonal rotation matrix which does not enter in the product $Y_W^t Y_W$ ($\mathcal{O}^t \mathcal{O} = I$) therefore it does not affect the study of LFV [45, 46]. Furthermore, elements of the A matrix are determined according to three possible scenarios: tau-electron, tau-muon and muon-electron. For the tau-electron (TE) scenario, we substitute $C_{\mu e} = C_{\tau\mu} = 0$ in equation (28) where $(\mathbf{n}_\mu, \mathbf{n}_e)$ and $(\mathbf{n}_\mu, \mathbf{n}_\tau)$ are orthogonal vectors. Thus we get:

$$Y_W^t Y_W = f^2 \begin{pmatrix} |n_e|^2 & 0 & \mathbf{n}_e \cdot \mathbf{n}_\tau \\ 0 & |n_\mu|^2 & 0 \\ \mathbf{n}_\tau \cdot \mathbf{n}_e & 0 & |n_\tau|^2 \end{pmatrix} \quad (30)$$

The Yukawa coupling matrix for the electron-tau scenario can be written as follows:

$$Y_{W_{\tau e}} = \mathcal{O} A_{\tau e} = \mathcal{O} f \begin{pmatrix} |n_e| & 0 & |n_\tau| C_{\tau e} \\ 0 & |n_\mu| & 0 \\ 0 & 0 & |n_\tau| \cdot \sqrt{1 - C_{\tau e}^2} \end{pmatrix} \quad (31)$$

By calculating the product $Y_W^t Y_W$, we get equation (30). In this case, the $A_{\tau e}$ matrix is written as follows:

$$A_{\tau e} = f \begin{pmatrix} |n_e| & 0 & |n_\tau| C_{\tau e} \\ 0 & |n_\mu| & 0 \\ 0 & 0 & |n_\tau| \cdot \sqrt{1 - C_{\tau e}^2} \end{pmatrix} \quad (32)$$

For the tau-muon (TM) scenario, we substitute $C_{\mu e} = C_{\tau e} = 0$ in equation (28) where $(\mathbf{n}_\mu, \mathbf{n}_e)$ and $(\mathbf{n}_e, \mathbf{n}_\tau)$ are orthogonal vectors. Thus, the matrix of Yukawa coupling can be written as follows:

$$Y_{W_{\tau\mu}} = \mathcal{O} A_{\tau\mu} = \mathcal{O} f \begin{pmatrix} |n_e| & 0 & 0 \\ 0 & |n_\mu| & |n_\tau| C_{\tau\mu} \\ 0 & 0 & |n_\tau| \cdot \sqrt{1 - C_{\tau\mu}^2} \end{pmatrix} \quad (33)$$

In this case, the $A_{\tau\mu}$ matrix is written as follows:

$$A_{\tau\mu} = f \begin{pmatrix} |n_e| & 0 & 0 \\ 0 & |n_\mu| & |n_\tau| C_{\tau\mu} \\ 0 & 0 & |n_\tau| \cdot \sqrt{1 - C_{\tau\mu}^2} \end{pmatrix} \quad (34)$$

While for the muon-electron (ME) scenario, we substitute $C_{\tau\mu} = C_{\tau e} = 0$ in equation (28) where $(\mathbf{n}_\mu, \mathbf{n}_\tau)$ and $(\mathbf{n}_\mu, \mathbf{n}_e)$ are orthogonal vectors. So, we get the matrix of Yukawa coupling in this case as follows:

$$Y_{W_{\mu e}} = \mathcal{O} A_{\mu e} = \mathcal{O} f \begin{pmatrix} |n_e| & \sqrt{1 - C_{\mu e}^2} & 0 & 0 \\ |n_e| C_{\mu e} & |n_\mu| & 0 \\ 0 & 0 & |n_\tau| \end{pmatrix} \quad (35)$$

In this case, the $A_{\mu e}$ matrix is written as follows:

$$A_{\mu e} = f \begin{pmatrix} |n_e| \sqrt{1 - C_{\mu e}^2} & 0 & 0 \\ |n_e| C_{\mu e} & |n_\mu| & 0 \\ 0 & 0 & |n_\tau| \end{pmatrix} \quad (36)$$

The TM scenario ($C_{\tau e} = C_{\mu e} = 0$) may produce large rates for τ - μ transitions, but always gives negligible contributions to $\text{LFV}_{\mu e}$ and $\text{LFV}_{\tau e}$. While the TE scenario ($C_{\tau\mu} = C_{\mu e} = 0$) may give sizable rates for the τ -e transitions, but always gives negligible contributions to $\text{LFV}_{\mu e}$ and $\text{LFV}_{\tau\mu}$. The ME scenario ($C_{\tau\mu} = C_{\tau e} = 0$) may produce large rates only for the μ -e transitions [46].

3 Z Boson LFV Decays ($Z \rightarrow l_i l_j$)

The Lagrangian of the lepton flavor violation (LFV) in Z boson decays can be written as follows [25, 47]:

$$\mathcal{L}_{Zl_i l_j} = \bar{l}_j [\gamma^\mu (A_1^L P_L + A_1^R P_R) + p^\mu (A_2^L P_L + A_2^R P_R)] l_i Z_\mu$$

Where $P_{L,R} = 1/2(1 \pm \gamma^5)$ are chirality projectors, l_i and l_j represent the lepton flavors and p is the 4-momentum for l_j . The coefficients $A_1^L, A_1^R, A_2^L, A_2^R$ can be obtained from the amplitudes of Feynman diagrams as shown in Fig.1. By neglecting the masses of charged leptons we can write the branching ratio equation of Z boson decays as follows [25, 47, 48]:

$$BR(Z \rightarrow l_i l_j) = BR(Z \rightarrow l_i \bar{l}_j) + BR(Z \rightarrow \bar{l}_i l_j) = \frac{\Gamma(Z \rightarrow l_i \bar{l}_j) + \Gamma(Z \rightarrow \bar{l}_i l_j)}{\Gamma_Z} \quad (37)$$

Γ_Z represents the total decay width of Z boson ($\Gamma_Z = 2.4952$ GeV) [56], while the decay width is given by [47, 48]:

$$\Gamma(Z \rightarrow l_i l_j) = \frac{m_Z}{48\pi} [2(|A_1^L|^2 + |A_1^R|^2) + \frac{m_Z^2}{4}(|A_2^L|^2 + |A_2^R|^2)] \quad (38)$$

Thus the final relation of the branching ratio can be written as follows:

$$BR(Z \rightarrow l_i l_j) = \frac{m_Z}{48\pi\Gamma_Z} [2(|A_1^L|^2 + |A_1^R|^2) + \frac{m_Z^2}{4}(|A_2^L|^2 + |A_2^R|^2)] \quad (39)$$

The coefficients $A_1^{L/R}$ and $A_2^{L/R}$ are combinations of the corresponding coefficients to each Feynman diagram as in Fig.1. Thus, they can be expressed as:

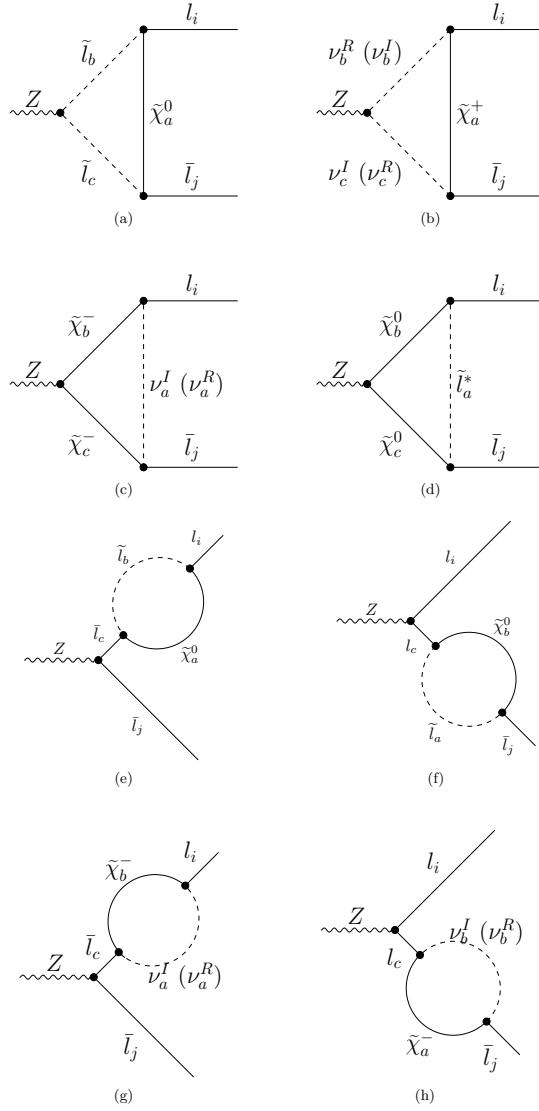


Fig. 1: One loop Feynman diagrams contributing to $\text{BR}(Z \rightarrow l_i \bar{l}_j)$ in the MSSM-Seesaw type-II model. These diagrams take more important role than the others.

$$A_1^{L/R} = A_{1a}^{L/R} + A_{1b}^{L/R} + A_{1c}^{L/R} + A_{1d}^{L/R} + A_{1e}^{L/R} + A_{1f}^{L/R} + A_{1g}^{L/R} + A_{1h}^{L/R}$$

$$A_2^{L/R} = A_{2a}^{L/R} + A_{2b}^{L/R} + A_{2c}^{L/R} + A_{2d}^{L/R} + A_{2e}^{L/R} + A_{2f}^{L/R} + A_{2g}^{L/R} + A_{2h}^{L/R}$$

The contributions of neutralino-slepton loops are derived from Fig.1(a, d, e, f), while the contributions of chargino-sneutrino loops are derived from Fig.1(b, c, g, h). The contributions of Fig.1(a, b) are:

$$A_1^{L(a,b)} = -2V_1^L V_2^R (-V_Z)C_{00} \quad (40)$$

$$A_2^{L(a,b)} = -2V_1^L V_2^L (-V_Z)(C_0 + C_1 + C_2)M \quad (41)$$

$$A_1^R = A_1^L (L \leftrightarrow R), A_2^R = A_2^L (L \leftrightarrow R) \quad (42)$$

The couplings corresponding to Fig.1(a) are: $V_1^L = \Gamma_{a,i,b}^{\tilde{\chi}^0 \tilde{l}^{*},L}$, which represents the left-handed coupling of the vertex neutralino-lepton-slepton ($\tilde{\chi}^0 - l - \tilde{l}^*$). $V_2^{L/R} = \Gamma_{j,a,c}^{\tilde{\chi}^0 \tilde{l}, L/R}$, which represents the left(right)-handed coupling of the vertex anti lepton-neutralino-slepton ($\tilde{\chi}^0 - l - \tilde{l}^*$). $V_Z = \Gamma_{c,b}^{\tilde{l} \tilde{l}^* Z}$, which represents coupling of the vertex slepton-slepton-Z boson ($\tilde{l} - \tilde{l}^* - Z$). The concrete forms of the previous couplings are available in the Appendix(A).

From equation (41) the M parameter represents the neutralino mass $m_{\tilde{\chi}_a^0}$. The parameters C_0, C_{00}, C_1 and C_2 represent the standard three-point functions, their definition is given in the LoopTools package [49, 50]. Thus, they can be calculated by a specific Mathematica package called Package-X [51]. The arguments of C functions from Fig.1(a) are $(0, m_Z^2, 0, m_{\tilde{\chi}_a^0}^2, m_{\tilde{l}_c}^2, m_{\tilde{l}_b}^2)$ where the external fermion masses have been set to zero.

The couplings corresponding to Fig.1(b) are: $V_1^L = \Gamma_{a,i,b}^{\tilde{\chi}^+ l \nu^{I/R}, L}$, which represents the left-handed coupling of the vertex chargino-lepton-(CP-odd/CP-even) sneutrino ($\tilde{\chi}^+ - l - \nu^{I/R}$). $V_2^{L/R} = \Gamma_{j,a,c}^{l \tilde{\chi}^- \nu^{I/R}, L/R}$, which represents the left(right)-handed coupling of the vertex lepton-chargino-(CP-odd/CP-even) sneutrino ($l - \tilde{\chi}^- - \nu^{I/R}$). $V_Z = \Gamma_{b,c}^{\nu^I \nu^R Z} = -\Gamma_{c,b}^{\nu^I \nu^R Z}$, which represents coupling of the vertex CP-odd sneutrino - CP-even sneutrino - Z boson ($\nu^I - \nu^R - Z$).

From equation (42) the M parameter represents the chargino mass $m_{\tilde{\chi}_a^\pm}$. The concrete forms of the above-mentioned couplings are available in the Appendix(A). The arguments of C functions from Fig.1(b) are $(0, m_Z^2, 0, m_{\tilde{\chi}_a^\pm}^2, m_{\nu_c^{R/I}}^2, m_{\nu_b^{I/R}}^2)$ where the

external fermion masses have been set to zero. The contributions of Fig.1(c,d) are:

$$A_1^{L(c,d)} = V_1^L V_2^R \left[V_Z^L C_0 m_1 m_2 - V_Z^R (B_0 - 2C_{00} + C_0) m_3^2 \right] \quad (43)$$

$$A_2^{L(c,d)} = 2V_1^L V_2^L \left[-V_Z^L C_1 m_1 + V_Z^R (C_0 + C_1 + C_2) m_2^2 \right] \quad (44)$$

$$\begin{aligned} A_1^R &= A_1^L (L \leftrightarrow R) \\ A_2^R &= A_2^L (L \leftrightarrow R) \end{aligned} \quad (45)$$

The couplings corresponding to Fig.1(c) are: $V_1^{L/R} = \Gamma_{b,i,a}^{\tilde{\chi}^+ l \nu^{J/R}, L/R}$, $V_2^{R/L} = \Gamma_{j,c,a}^{\tilde{l} \tilde{\chi}^- \nu^{J/R}, R/L}$ and $V_Z^{L/R} = \Gamma_{c,b}^{\tilde{\chi}^+ \tilde{\chi}^- Z, L/R}$ which represents the coupling of the vertex chargino-chargino-Z boson ($\tilde{\chi}^+ - \tilde{\chi}^- - Z$). The m_1, m_2 and m_3 parameters represent the masses of chargino and (CP-odd/CP-even) sneutrino ($m_{\tilde{\chi}_b^-}, m_{\tilde{\chi}_c^-}, m_{\nu_a^{I/R}}$) respectively. The concrete forms of the couplings are available in the Appendix(A). The arguments of C functions from Fig.1(c) are $(m_Z^2, 0, 0, m_{\tilde{\chi}_c^-}^2, m_{\tilde{\chi}_b^-}^2, m_{\nu_a^{I/R}}^2)$ where the external fermion masses have been set to zero. B_0 is a two-point function and its arguments are $(m_Z^2, m_{\tilde{\chi}_b^-}^2, m_{\tilde{\chi}_c^-}^2)$.

The couplings corresponding to Fig.1(d) are: $V_1^L = \Gamma_{b,i,a}^{\tilde{\chi}^0 \tilde{l}^*, L}$, $V_2^{R/L} = \Gamma_{j,c,a}^{\tilde{l} \tilde{\chi}^0, R/L}$ and $V_Z^{L/R} = \Gamma_{c,b}^{\tilde{\chi}^0 \tilde{\chi}^0 Z, L/R}$ which represents coupling of the vertex neutralino-neutralino-Z boson ($\tilde{\chi}^0 - \tilde{\chi}^0 - Z$). The concrete forms of the couplings are available in the Appendix(A). The m_1, m_2 and m_3 parameters represent the masses of neutralino and slepton ($m_{\tilde{\chi}_b^0}, m_{\tilde{\chi}_c^0}, m_{\tilde{l}_a}$) respectively. The arguments of C functions from Fig.1(d) are $(m_Z^2, 0, 0, m_{\tilde{\chi}_c^0}^2, m_{\tilde{\chi}_b^0}^2, m_{\tilde{l}_a}^2)$ where the external fermion masses have been set to zero. The arguments of B function are $(m_Z^2, m_{\tilde{\chi}_b^0}^2, m_{\tilde{\chi}_c^0}^2)$.

The contributions of Feynman diagrams Fig.1(e, f, g, h), here Z boson doesn't couple to a scalar particle therefore $A_2^{L/R} = 0$, can be written as follows:

$$A_1^L = \frac{V_Z^L}{m_1^2 - m_2^2} \left[-V_1^L V_2^R B_1 m_1^2 + V_1^R V_2^R B_0 m_1 m_3 - V_1^R V_2^L B_1 m_1 m_2 + V_1^L V_2^L B_0 m_3 m_2 \right] \quad (46)$$

$$A_1^R = A_1^L (L \leftrightarrow R) \quad (47)$$

The couplings corresponding to Fig.1(e) are: $V_1^{L/R} = \Gamma_{a,i,b}^{\tilde{\chi}^0 \tilde{l}^*, L/R}$, $V_2^{R/L} = \Gamma_{a,i,b}^{\tilde{l} \tilde{\chi}^0, R/L}$ and $V_Z^L = \Gamma_{j,c}^{\tilde{l} \tilde{l} Z, L}$ which represents the left-handed coupling of the vertex anti lepton-lepton-Z boson ($\tilde{l} - l - Z$). The m_1, m_2 and m_3 parameters represent the masses of

leptons and neutralino $(m_{l_i}, m_{l_c}, m_{\tilde{\chi}_a^0})$, respectively. The arguments of B functions are $(m_{l_i}^2, m_{\tilde{\chi}_a^0}^2, m_{l_b}^2)$.

The couplings corresponding to Fig.1(f) are: $V_1^{L/R} = \Gamma_{b,c,a}^{\tilde{\chi}^0 \tilde{l}^*, L/R}$, $V_2^{R/L} = \Gamma_{j,b,a}^{\tilde{l} \tilde{\chi}^0, R/L}$ and $V_Z^L = \Gamma_{c,i}^{\tilde{l} Z, L}$. Here m_1, m_2 and m_3 parameters represent the masses of $(m_{l_j}, m_{l_c}, m_{\tilde{\chi}_b^0})$ respectively. The arguments of B functions are $(m_{l_j}^2, m_{\tilde{\chi}_b^0}^2, m_{l_a}^2)$.

The couplings corresponding to Fig.1(g) are: $V_1^{L/R} = \Gamma_{b,i,a}^{\tilde{\chi}^+ \tilde{l} \nu^{I/R}, L/R}$, $V_2^{R/L} = \Gamma_{c,b,a}^{\tilde{l} \tilde{\chi}^- \nu^{I/R}, R/L}$ and $V_Z^L = \Gamma_{j,c}^{\tilde{l} Z, L}$. Where m_1, m_2 and m_3 parameters represent the masses of leptons and chargino $(m_{l_i}, m_{l_c}, m_{\tilde{\chi}_b^-})$, respectively. The arguments of B functions are $(m_{l_i}^2, m_{\tilde{\chi}_b^-}^2, m_{\nu_a^{I/R}}^2)$.

The couplings corresponding to Fig.1(h) are: $V_1^{L/R} = \Gamma_{a,c,b}^{\tilde{\chi}^+ \tilde{l} \nu^{I/R}, L/R}$, $V_2^{R/L} = \Gamma_{j,a,b}^{\tilde{l} \tilde{\chi}^- \nu^{I/R}, R/L}$ and $V_Z^L = \Gamma_{c,i}^{\tilde{l} Z, L}$. Where m_1, m_2 and m_3 parameters represent the masses of leptons and chargino $(m_{l_j}, m_{l_c}, m_{\tilde{\chi}_a^-})$, respectively. The arguments of B functions are $(m_{l_j}^2, m_{\tilde{\chi}_a^-}^2, m_{\nu_b^{I/R}}^2)$. The concrete forms of the couplings are available in the Appendix(A).

4 Numerical Results and Discussion

In this section, the numerical results are implemented using the SARAH, SPheno and FlavorKit packages [52–55]. SARAH package is a Mathematica package for building and analyzing SUSY and non-SUSY models. It creates source code for Spheno tool. SPheno stands for S(upsymmetric) Pheno(menology). The SPheno code is written in Fortran-90 and it calculates the SUSY spectrum using low energy data and a user supplied high scale model as input like MSSM, type-I seesaw (type-II and type-III seesaw), NMSSM and other models. Furthermore, the FlavorKit package which is included in SARAH can compute a wide range of flavor observables like LFV in Z boson, Higgs and lepton decays [47].

According to the considered CMSSM-Seesaw type-III model, the final parameters in this work are: Y_W , M_W , f , $|n_e|$, $|n_\mu|$, $|n_\tau|$, $C_{\tau\mu}$, $C_{\tau e}$, $C_{\mu e}$, $m_{1/2}$, m_0 , A_0 , $\tan\beta$, and $\text{sign}(\mu)$. In our calculations the soft symmetry breaking terms are constrained by several theoretical and experimental conditions. Such as the conservation of R-parity and the lightest SUSY particle of the studied model is the neutralino. Furthermore, the SUSY particle masses (charginos, neutralinos, sleptons and sneutrinos) which are calculated with SPheno must be above the recent experimental mass limits [56], as shown in table 4.

The SUSY particle masses are related to both $m_{1/2}$ and m_0 . Therefore, we firstly determine their minimum values according to the previous conditions, so $m_{1/2} =$ and $m_0 = 500$ GeV. The parameters space for both $\tan\beta$ and A_0 are determined for obtaining numerical results by running SPheno without any error. Errors typically occur for two main reasons: (i) Out of the values range of A_0 and $\tan(\beta)$, the gauge couplings become large at M_{GUT} due to large beta functions. Hence, the perturbation

Table 4: Experimentally mass limits of SUSY particles [56].

Sparticle	Mass limits (GeV)
Sleptons	> 107
Sneutrinos	> 94
Neutralinos	> 46
Charginos	> 94

theory will fail. (ii) Negative mass square for the SUSY particles [37]. The values of input parameters are then shown in table 5.

Table 5: The input parameters values range in this study.

Parameter	Values
m_0 (GeV)	[500,1500]
$m_{1/2}$ (GeV)	[500,1000]
A_0 (GeV)	[-1700,1850]
$\tan\beta$	[5,20]
$\cos(\theta_{ij})$	[0.087,0.91]

From equations (24, 31, 33, 35), we can estimate both values of the Yukawa matrix elements Y_W (Yukawa couplings) and the triplet fermion mass M_W according to the mass limit condition for the light neutrino which is estimated to be < 0.8 eV at low energy scale [8]. By inverting the equation (24), for any fixed values of the light neutrino masses we can guess the Yukawa matrix elements as a function of the corresponding M_W for any fixed value of the Yukawa couplings. This guess will not provide the correct values of the Yukawa couplings, because the neutrino masses are measured at low energy, in order to calculate the neutrino masses (m_ν) from equation (24) we should insert values of M_W and Y_W parameters at the high energy scale. However, this guess can be used to run the RGEs numerically to obtain the exact light neutrino masses at low energy for these input parameters. The difference between these results can be obtained numerically, so the input numbers can be minimized in an iterative procedure until the convergence is achieved. Provided that the Yukawa matrix elements $|(Y_W)_{ij}| < 1$ [37], the convergence can be reached in several steps.

In this study, we consider sizable values for the Yukawa matrix elements. Thus, we should check that they are still within the perturbation regime. Hence, the constraint on the maximum allowed values of entries for the Yukawa matrix is chosen to be: $|(Y_W)_{ij}|^2 < 4\pi$ [45]. So we get $M_W \geq 2.5 \times 10^{13}$ GeV and $\cos(\theta_{ij}) \leq 0.91$. $\text{sign}(\mu) > 0$ is fixed for all numerical calculations. From equations (31, 33, 35) we can get three scenarios of the Yukawa coupling matrix for the Z boson LFV decays. The values of $|n_e|$, $|n_\mu|$ and $|n_\tau|$ are set as shown in table 6.

The energy scale of the GUT is fixed to $M_{GUT} = 2.00 \times 10^{16}$ GeV. While the SUSY breaking scale is fixed to $M_{SUSY} = 10^3$ GeV [57]. The $\text{BR}(Z \rightarrow l_i l_j)$ will be studied with(without) applying the constraints due to non-observation of the $l_i \rightarrow l_j \gamma$ decays.

Table 6: Yukawa matrix scenarios for numerical calculations of $\text{BR}(Z \rightarrow l_i l_j)$.

Scenario	$C_{\tau\mu}$	$C_{\tau e}$	$C_{\mu e}$	$ n_e $	$ n_\mu $	$ n_\tau $	Yukawa matrix
TM	$C_{\tau\mu}$	0	0	0.001	1	1	$Y_W = f \begin{pmatrix} 0.001 & 0 & 0 \\ 0 & 1 & C_{\tau\mu} \\ 0 & 0 & \sqrt{1 - C_{\tau\mu}^2} \end{pmatrix}$
TE	0	$C_{\tau e}$	0	1	0.001	1	$Y_W = f \begin{pmatrix} 1 & 0 & C_{\tau e} \\ 0 & 0.001 & 0 \\ 0 & 0 & \sqrt{1 - C_{\tau e}^2} \end{pmatrix}$
ME	0	0	$C_{\mu e}$	1	1	0.001	$Y_W = f \begin{pmatrix} \sqrt{1 - C_{\mu e}^2} & 0 & 0 \\ C_{\mu e} & 1 & 0 \\ 0 & 0 & 0.001 \end{pmatrix}$

4.1 $\text{BR}(Z \rightarrow l_i l_j)$ without constraints on $(l_i \rightarrow l_j \gamma)$ decays

In this section, we consider the case of the $\text{BR}(Z \rightarrow l_i l_j)$ as a function of A_0 , $\tan(\beta)$, M_W and $\cos(\theta_{ij})$. The A_0 and $\cos(\theta_{ij})$ parameters are present in non-diagonal elements of the left sleptons mass matrix and tri-linear coupling terms as shown in equation (26). The effects of $\cos(\theta_{ij})$ in numerical results arise from the product $Y_W^t Y_W$. In RGEs, Δm_L^2 and ΔT_l^2 are proportional to A_0^2 , A_0 and $(Y_W^t Y_W)_{ij} = f^2 n_i n_j \cos(\theta_{ij})$ where i, j indicate to the neutrino generation. The Y_W matrix and M_W parameter are also related to Weinberg operator which is in turn related to the mass matrix of CP-even and CP-odd sneutrino as shown in equations (9, 11). Thus, the contributions from sneutrino-chargino can be influenced by elements of the Y_W matrix and values of the triplet mass M_W . Variations of $\text{BR}(Z \rightarrow l_i l_j)$ as a function of $\cos(\theta_{ij})$ also as a contour of A_0 and $\tan\beta$ are studied as shown in Fig.2.

Fig.2 shows in the left side that BRs of Z decays increase as values of $\cos(\theta_{ij})$ vary from 0.087 to 0.91 for these two cases $A_0 = 0, 1850$ GeV and $\tan\beta=5, 20$. For $A_0 = 1850$ GeV and $\tan\beta=20$ we get the best value of $\text{BR}(Z \rightarrow \tau l)$ (red line). While the best values of $\text{BR}(Z \rightarrow \mu e)$ are at $A_0 = 1850$ GeV and $\tan\beta=5, 20$ (dashed-black and red lines). Furthermore, we notice that $\text{BR}(Z \rightarrow \mu e) = \text{BR}(Z \rightarrow \tau l)$ at two cases, when $A_0 = 0$ GeV, $\tan\beta=5, 20$ and $A_0 = 1850$ GeV, $\tan\beta=5$.

Fig.2 shows in the right side the $\text{BR}(Z \rightarrow l_i l_j)$ as a contour of A_0 and $\tan\beta$ at $\cos(\theta_{ij})=0.91$. It is obvious that the values of $\text{BR}(Z \rightarrow l_i l_j)$ increase by increasing the absolute values of A_0 at any fixed value of $\tan\beta$. This means that the sign of A_0 has no considerable effect on the prediction of BRs of the Z boson LFV decays. However, the sign of A_0 is still relevant to the precise prediction. It is also clear that the variation of $\text{BR}(Z \rightarrow l_i l_j)$ is very small when $5 \leq \tan\beta \leq 20$ at a fixed value of A_0 . This means that the presence of A_0 and $\cos(\theta_{ij})$ in RGEs increases the branching ratios of $Z \rightarrow l_i l_j$. While the dependence of the Z boson LFV decays on $\tan\beta$ is weak so that $\tan\beta$ is not embedded in RGEs.

Furthermore, we notice that $1.5 \times 10^{-11} \leq \text{BR}(Z \rightarrow \mu e) \leq 5.5 \times 10^{-10}$ when $5 \leq \tan\beta \leq 20$ at $-1700 \leq A_0 \leq 1850$ GeV. For the other two decay channels it is obvious that $\text{BR}(Z \rightarrow \tau e) = \text{BR}(Z \rightarrow \tau \mu)$ where $3.5 \times 10^{-12} \leq \text{BR}(Z \rightarrow \tau l) \leq 1 \times 10^{-9}$ when $5 \leq \tan\beta \leq 20$ and $-1700 \leq A_0 \leq 1850$ GeV. The best values of $\text{BR}(Z \rightarrow l_i l_j)$ are at both $\tan\beta = 20$ and $A_0 = 1850$ GeV (red region). Thus, we fix $\tan\beta = 20$ and $A_0 = 1850$ GeV for the next calculations.

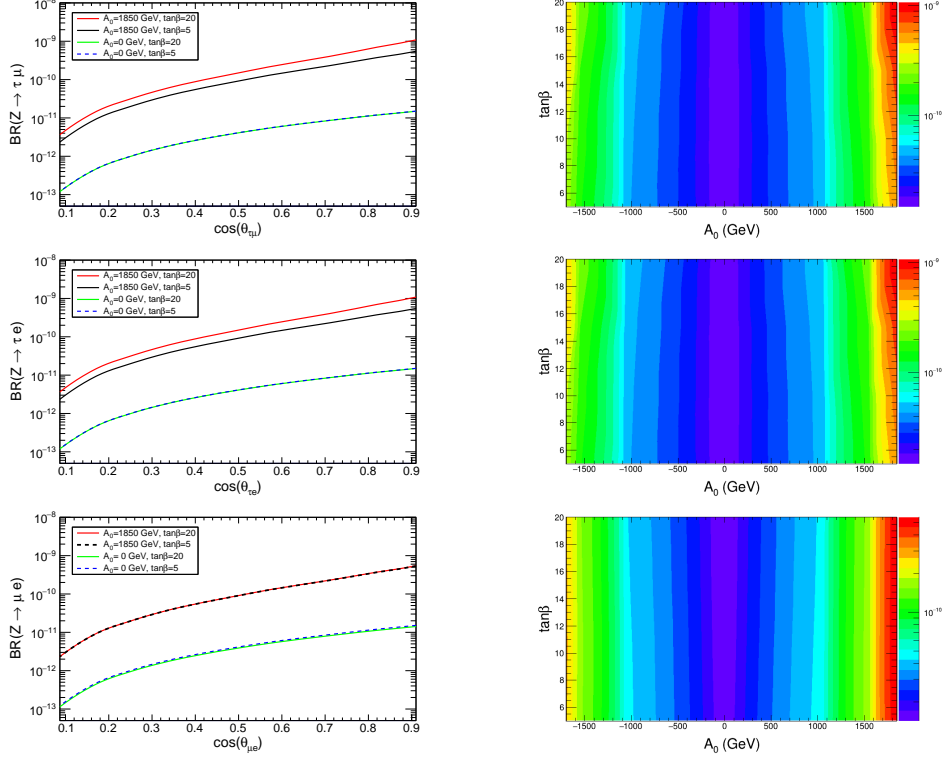


Fig. 2: BR($Z \rightarrow l_i l_j$) as a function of $\cos(\theta_{ij})$ at $A_0 = 0, 1850$ GeV and $\tan\beta=5, 20$ (left). BR($Z \rightarrow l_i l_j$) as a contour in the A_0 and $\tan\beta$ plane at $\cos(\theta_{ij})=0.91$ (Right). For all above plots we set $m_{1/2}=m_0 = 500$ GeV, $f = 1$ and $M_W = 2.5 \times 10^{13}$ GeV.

We plot BR($Z \rightarrow l_i l_j$) versus strength of the neutrino Yukawa coupling (f) for these two values of $M_W = 2.5 \times 10^{13}/2.5 \times 10^{14}$ GeV as shown in Fig.3. The red line denotes BR($Z \rightarrow \mu e$), the black one denotes BR($Z \rightarrow \tau e$) and the dashed-green one denotes BR($Z \rightarrow \tau\mu$). We notice that at $M_W = 2.5 \times 10^{13}$ GeV, the values of BRs of the Z boson LFV decays increase as the values of the f parameter vary from 0.2 to 1. However, at $f=0.85$ the BRs of the Z boson LFV decays have the best values then these values slowly decrease as the f parameter increases from 0.85 to 1. At $f=0.85$ the BR($Z \rightarrow \tau l$) is about 1.30×10^{-9} and BR($Z \rightarrow \mu e$) is about 6.40×10^{-10} . While at $M_W = 2.5 \times 10^{14}$ GeV, the values of the BRs of the Z boson LFV decays increase as the f parameter varies from 0.1 to 1.

At $M_W = 2.5 \times 10^{13}$ GeV the values of BRs are better than at $M_W = 2.5 \times 10^{14}$ GeV. At $M_W = 2.5 \times 10^{13}$ GeV the range of BR($Z \rightarrow \mu e$) is $[2.7 \times 10^{-12}, 5.5 \times 10^{-10}]$ and for BR($Z \rightarrow \tau l$) is $[3.5 \times 10^{-10}, 1.27 \times 10^{-9}]$. While at $M_W = 2.5 \times 10^{14}$ GeV we notice that BR($Z \rightarrow \tau l$) \simeq BR($Z \rightarrow \mu e$), where the range of BR($Z \rightarrow \mu e$) is $[4.5 \times 10^{-15}, 1.5 \times 10^{-11}]$ and for BR($Z \rightarrow \tau l$) is $[5.5 \times 10^{-15}, 1.9 \times 10^{-11}]$.

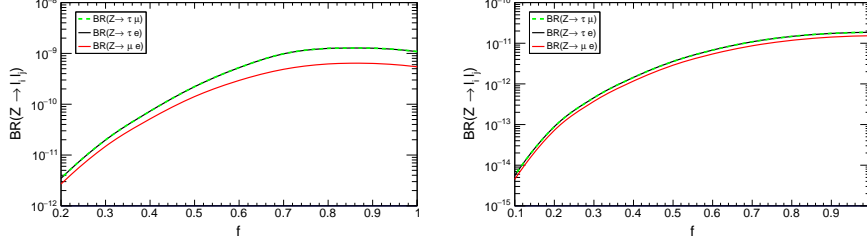


Fig. 3: $\text{BR}(Z \rightarrow l_i l_j)$ as a function of the strength of neutrino Yukawa coupling (f) at two values of $M_W = 2.5 \times 10^{13}$ GeV (left), and 2.5×10^{14} GeV (right). $\text{BR}(Z \rightarrow \tau\mu)$ in dashed-green line, $\text{BR}(Z \rightarrow \tau e)$ in black one and $\text{BR}(Z \rightarrow \mu e)$ in red one. Where the other input parameter are fixed as $m_0 = m_{1/2} = 500$ GeV, $A_0 = 1850$ GeV, $\tan\beta=20$ and $\cos(\theta_{ij})=0.91$.

We also consider the case of the $\text{BR}(Z \rightarrow l_i l_j)$ as a contour in the m_0 and $m_{1/2}$ plane. The m_0 parameter is related to the soft breaking slepton mass terms $m_{\tilde{L}}$ and the mass matrices of sleptons, CP-odd and CP-even sneutrinos. The $m_{1/2}$ parameter is related to the soft breaking gaugino mass terms and the mass matrices of both neutralino and chargino. Thus, both m_0 and $m_{1/2}$ can induce the contributions from neutralino-slepton and sneutrino-chargino.

We plot $\text{BR}(Z \rightarrow l_i l_j)$ as a contour in the m_0 and $m_{1/2}$ plane as shown in Fig.4. In this case other input parameters are fixed as follows : $A_0 = 1850$ GeV, $\tan \beta = 20$, $\cos(\theta_{ij}) = 0.91$, $f=0.85$ and $M_W = 2.5 \times 10^{13}$ GeV. We notice that the $\text{BR}(Z \rightarrow l_i l_j)$

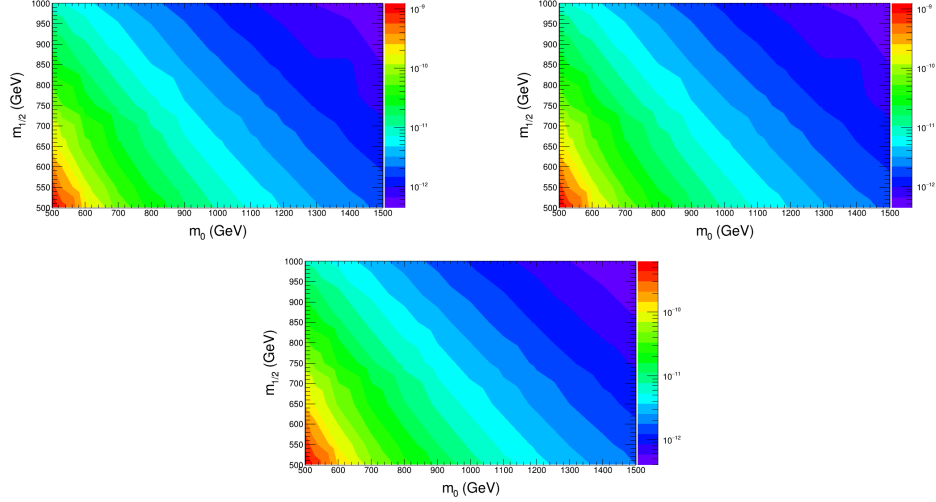


Fig. 4: $\text{BR}(Z \rightarrow l_i l_j)$ as a contour in the m_0 and $m_{1/2}$ plane. $\text{BR}(Z \rightarrow \tau\mu)$ shown in upper-left figure, $\text{BR}(Z \rightarrow \tau e)$ shown in upper-right one and $\text{BR}(Z \rightarrow \mu e)$ shown in bottom one. Best values of $\text{BR}(Z \rightarrow l_i l_j)$ for all decay channels are in red region.

decreases by increasing both m_0 and $m_{1/2}$. This means that the Z boson LFV decays depend strongly on m_0 and $m_{1/2}$. The best values of BRs are at $m_0 = [500, 520]$ GeV and $m_{1/2} = [500, 530]$ GeV (red region). Thus, the Z boson LFV decays can occur at the low mass limit of the SUSY particles where their masses increase by increasing both m_0 and $m_{1/2}$. Moreover, the contributions of non-diagonal elements of the slepton mass matrices in the Z boson LFV decays decrease by increasing m_0 . This indicates that large values of m_0 and $m_{1/2}$ suppress the LFV of Z boson decays. The best value of $\text{BR}(Z \rightarrow \tau l)$ is about 1.30×10^{-9} and $\text{BR}(Z \rightarrow \mu e)$ is about 6.4×10^{-10} .

Regarding the Yukawa couplings scenarios and the mass limits of the SUSY particles, the branching ratios for $(l_i \rightarrow l_j \gamma)$ decays are quite large so that they do not respect the experimental limits as shown in table 7. Hence, the previous plots give the maximum values that $\text{BR}(Z \rightarrow l_i l_j)$ can reach in the MSSM-Seesaw-III model without applying the constraints on these decays.

4.2 $\text{BR}(Z \rightarrow l_i l_j)$ with constraints on $(l_i \rightarrow l_j \gamma)$ decays

In this section, we study the variations of $\text{BR}(Z \rightarrow l_i l_j)$ after applying constraints on $\text{BR}(l_i \rightarrow l_j \gamma)$. The $l_i \rightarrow l_j \gamma$ decays are not observed in any experiment. Hence, the branching ratios for these decays are constrained as shown in table 7. In the supersym-

Decay	Upper Limit	Experiment
$BR(\tau \rightarrow \mu \gamma)$	4.2×10^{-8} [58]	Belle
$BR(\tau \rightarrow e \gamma)$	5.6×10^{-8} [58]	Belle
$BR(\mu \rightarrow e \gamma)$	4.2×10^{-13} [59]	MEG

Table 7: Experimental upper limits of the lepton flavor violating radiative two body decays $(l_i \rightarrow l_j \gamma)$.

metry, the source of LFV processes can be non-diagonal elements in the left slepton mass matrix. Therefore, in the mass insertion method (MI) with leading-logarithm approximation, the branching ratios of the $l_i \rightarrow l_j \gamma$ decays can be approximated as follows [37, 39]:

$$BR(l_i \rightarrow l_j \gamma) \propto \alpha^3 m_{l_i}^5 \frac{|\Delta m_{L_{ij}}^2|^2}{\tilde{m}^8} \tan^2(\beta) \quad (48)$$

Where α is the electroweak coupling constant, m_{l_i} is the mass of lepton i and \tilde{m} is the average of SUSY masses that are involved in loops.

From the above-mentioned study (section 4.1) we found that the branching ratios for the $l_i \rightarrow l_j \gamma$ decays are quite large. However, this does not completely exclude the MSSM-Seesaw type-III model since there are certain parameter regions where cancellations between different contributions can occur. From equations (26, 48), we notice that $\text{BR}(l_i \rightarrow l_j \gamma)$ are mainly related to the SUSY mass scale and elements of the non-diagonal left slepton mass matrix. The non-diagonal elements are almost completely governed by the choice of soft SUSY breaking parameters in the heavy

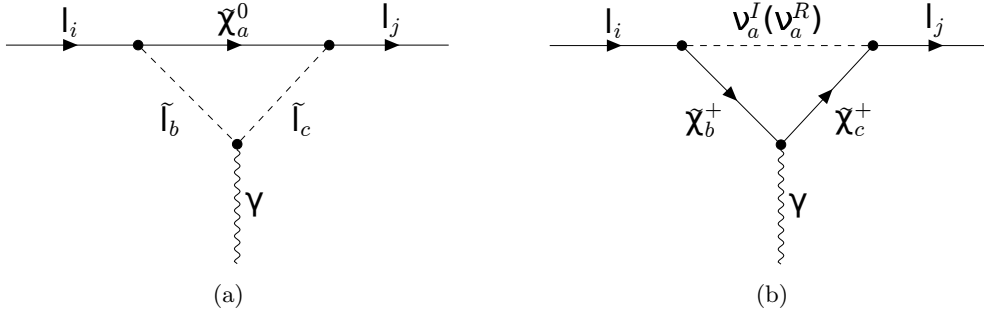


Fig. 5: One loop Feynman diagrams contributing to $\text{BR}(l_i \rightarrow l_j \gamma)$ in the MSSM-Seesaw type-III model.

seesaw sector. Furthermore, $\text{BR}(l_i \rightarrow l_j \gamma)$ is proportional to the square of $\tan\beta$ which leads to larger LFV branching ratios. Therefore, we fixed $A_0 = 0$ GeV (to exclude trilinear couplings) and $\tan\beta=5$ for all calculations. While we fixed $m_0 = m_{1/2} = 500$ GeV by considering the conditions of mass limits for the SUSY particles as shown in table 4. We will utilize the LFV of the $l_i \rightarrow l_j \gamma$ decays to constrain the f parameter, while the values of the Y_W matrix elements are fixed as shown in table 6. The sparticles mediated diagrams (sleptons, sneutrinos, neutralinos and charginos) for the $l_i \rightarrow l_j \gamma$ decays in the MSSM-Seesaw type-III model are shown in Fig.5. The off-shell amplitude for $(l_i \rightarrow l_j \gamma)$ is given by [47, 60]:

$$M = e\epsilon^{\alpha*} \bar{u}_i(p-q) [q^2 \gamma_\alpha (K_1^L P_L + K_1^R P_R) + m_{l_i} i \sigma_{\alpha\beta} q^\beta (K_2^L P_L + K_2^R P_R)] u_j(p) \quad (49)$$

Here q represents the momentum of photon. e is the electric charge, ϵ^α is the polarization vector of photon, u_i and u_j represent the wave function for anti-lepton/lepton and p is momentum of the lepton l_i . In the limit $q \rightarrow 0$, the analytic expression of the branching ratio of the $(l_i \rightarrow l_j \gamma)$ decays is:

$$\text{BR}(l_i \rightarrow l_j \gamma) = \alpha \frac{m_{l_i}^5}{\Gamma_{l_i}} (|K_2^L|^2 + |K_2^R|^2) \quad (50)$$

Where α is the fine structure constant and Γ_{l_i} is the total decay width of l_i . $K_2^{L/R}$ are the combinations of the coefficients which correspond to Feynman diagrams as in Fig.5 and could be written as:

$$K_2^{L/R} = K_{2a}^{L/R} + K_{2b}^{L/R} \quad (51)$$

Here the contributions from neutralino-slepton loops are shown in Fig.5(a). While the contributions from chargino-sneutrino loops are shown in Fig.5(b). The contribution

of Fig.5(a) is given by:

$$K_2^L = 2V_\gamma [V_1^L V_2^R (C_2 + C_{12} + C_{11}) m_{e_i} + V_1^R V_2^L (C_1 + C_{12} + C_{11}) m_{e_j} - V_1^R V_2^R (C_0 + C_1 + C_2) m_{\tilde{\chi}_a^0}] \quad (52)$$

$$K_2^R = K_2^L (L \leftrightarrow R) \quad (53)$$

The couplings corresponding to Fig.5(a) are: $V_\gamma = \Gamma_{c,b}^{\tilde{u}^* \gamma}$ which represents the coupling of vertex slepton-slepton-gamma, $V_1^{(L/R)} = \Gamma_{i,a,b}^{\tilde{\chi}^0 \tilde{l},(L/R)}$ which represents the left(right)-handed coupling of vertex anti lepton-neutralino-slepton, and $V_2^{(L/R)} = \Gamma_{a,j,c}^{\tilde{\chi}^0 \tilde{u}^*,(L/R)}$ which represents the left(right)-handed coupling of vertex neutralino-lepton-slepton. The concrete forms of couplings are included in the Appendix A. While $C_0, C_{00}, C_1, C_2, C_{11}, C_{12}$ are the standard three-point functions with their definition given in the LoopTools program [49, 50], and it can be calculated by the Mathematica package Package-X [51]. The arguments of the C functions with vanishing external momenta of Fig.5(a) are $(m_{\tilde{\chi}_a^0}^2, m_{\tilde{l}_c}^2, m_{\tilde{l}_b}^2)$. The contribution of Fig.5(b) is given by:

$$K_2^L = -2(V_\gamma^L)^* V_1^L V_2^R C_{12} m_{e_i} + 2(V_\gamma^R)^* V_1^R V_2^L (C_2 + C_{12} + C_{22}) m_{e_j} + 2(V_\gamma^L)^* V_1^R V_2^R C_1 m_{\tilde{\chi}_b^-} - 2(V_\gamma^R)^* V_1^R V_2^R (C_0 + C_1 + C_2) m_{\tilde{\chi}_c^-} \quad (54)$$

$$K_2^R = K_2^L (L \leftrightarrow R) \quad (55)$$

The couplings corresponding to Fig.5(b) are $V_\gamma^{(L/R)} = \Gamma_{b,c}^{\tilde{\chi}^+ \tilde{\chi}^- \gamma,(L/R)}$ which represents the left(right)-handed coupling of vertex chargino-chargino-gamma, $V_1^{(L/R)} = \Gamma_{i,b,a}^{\tilde{\chi}^- \nu^I,(L/R)}$ which represents the left(right)-handed coupling of vertex anti lepton-chargino- CP-odd sneutrino, and $V_2^{(L/R)} = \Gamma_{c,j,a}^{\tilde{\chi}^+ \nu^I,(L/R)}$ which represents the left(right)-handed coupling of vertex chargino-lepton- CP-even sneutrino. The concrete forms of couplings are included in the Appendix A. While $C_0, C_1, C_2, C_{12}, C_{22}$ are the standard three-point functions. The arguments of C functions with vanishing external momenta from Fig.5(b) are $(m_{\tilde{\chi}_c^-}^2, m_{\tilde{\chi}_b^-}^2, m_{\nu_a^I}^2)$. For the CP-even sneutrino couplings we replace ν^I with ν^R in the last two vertices $V_1^{(L/R)}, V_2^{(L/R)}$ and the arguments of C functions.

After studying the analytical expression of $\text{BR}(l_i \rightarrow l_j \gamma)$, we start the numerical discussion with μ decays since its experimental limits are the most stringent. By taking $m_0 = m_{1/2} = 500$ GeV, $\tan\beta=5$, $M_W = 2.5 \times 10^{13}$ GeV and $A_0 = 0$ GeV, we plot $\text{BR}(\mu \rightarrow e \gamma)$ versus the f parameter and $\text{BR}(Z \rightarrow \mu e)$ versus f at $\cos(\theta_{\mu e}) = 0.91, 0.57$ and 0.17 as shown in Fig.6. The horizontal dotted blue line represents the current experimental limit of $\text{BR}(\mu \rightarrow e \gamma)$ as shown in table 7. It is obvious that both $\text{BR}(\mu \rightarrow e \gamma)$ and $\text{BR}(Z \rightarrow \mu e)$ increase as the f parameter varies from 0.001 to 0.1. The prediction of $\text{BR}(\mu \rightarrow e \gamma)$ exceeds the current experimental limit at $f = 0.0151, 0.0195$ and 0.035 in red line, black and green one respectively. So in this case the $\text{BR}(Z \rightarrow \mu e)$ is $4.00 \times 10^{-18}, 4.14 \times 10^{-18}$ and 4.16×10^{-18} at $f = 0.015$ ($\cos(\theta_{\mu e})=0.91$), 0.0195 ($\cos(\theta_{\mu e})=0.57$) and 0.035 ($\cos(\theta_{\mu e})=0.17$) respectively. Thus, under constraints

of the $\mu \rightarrow e\gamma$ decay the value of $\text{BR}(Z \rightarrow \mu e)$ is approximately 4.00×10^{-18} . This predicted value is eleven orders of magnitude below the current experimental limit and eight orders of magnitude below the future experiment sensitivity as shown in table 1. These numerical results indicate that when $\cos(\theta_{\mu e})$ increases the value of f is constrained to be small and the predicted values of $\text{BR}(Z \rightarrow \mu e)$ are approximately equal for these values of $\cos(\theta_{\mu e})=0.91, 0.57$ and 0.17 .

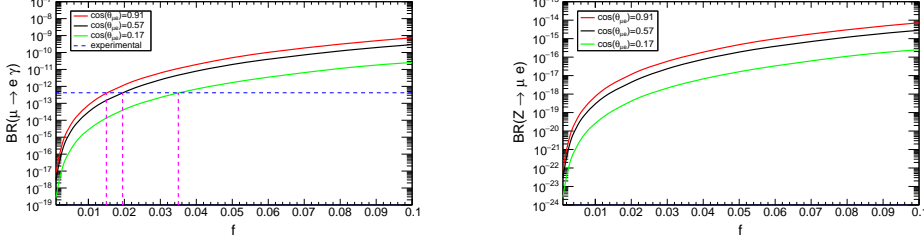


Fig. 6: $\text{BR}(\mu \rightarrow e\gamma)$ versus f (left), $\text{BR}(Z \rightarrow \mu e)$ versus f (right). For these two plots we set $\cos(\theta_{\mu e})=0.91$ in red line, $\cos(\theta_{\mu e})=0.57$ in black one and $\cos(\theta_{\mu e})=0.17$ in green one.

In Fig.7, we plot $\text{BR}(\tau \rightarrow \mu\gamma)$ versus the f parameter and $\text{BR}(Z \rightarrow \tau\mu)$ versus f at $\cos(\theta_{\tau\mu}) = 0.91, 0.57$ and 0.17 . The horizontal dotted blue line represents the current experimental limit of $\text{BR}(\tau \rightarrow \mu\gamma)$ as shown in table 7. We notice that both $\text{BR}(\tau \rightarrow \mu\gamma)$ and $\text{BR}(Z \rightarrow \tau\mu)$ increase as the f parameter varies from 0.1 to 1. The prediction of $\text{BR}(\tau \rightarrow \mu\gamma)$ exceeds the current experimental limit at $f = 0.532, 0.85$ and 1 in red line, black and green one respectively. So, in this case the $\text{BR}(Z \rightarrow \tau\mu)$ is $3.26 \times 10^{-12}, 4.00 \times 10^{-12}$ and 4.65×10^{-13} at $f = 0.532$ ($\cos(\theta_{\tau\mu})=0.91$), 0.85 ($\cos(\theta_{\tau\mu})=0.57$) and 1 ($\cos(\theta_{\tau\mu})=0.17$) respectively. Thus, under constraints of the $\tau \rightarrow \mu\gamma$ decay, the best predicted value of $\text{BR}(Z \rightarrow \tau\mu)$ is approximately 4.00×10^{-12} . The predicted value is six orders of magnitude below the current experimental limit and four orders of magnitude below the future experiments sensitivity as shown in table 1.

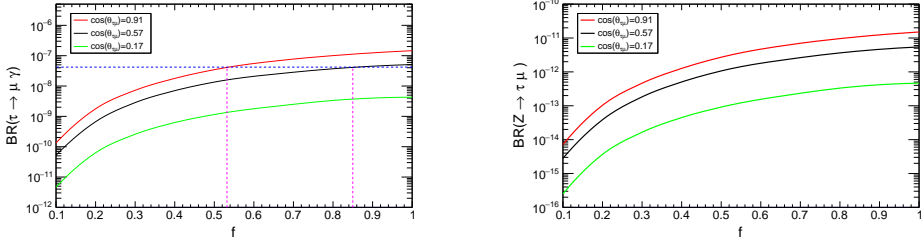


Fig. 7: $\text{BR}(\tau \rightarrow \mu\gamma)$ versus f (left), $\text{BR}(Z \rightarrow \tau\mu)$ versus f (right). For these two plots we set $\cos(\theta_{\tau\mu})=0.91$ in red line, $\cos(\theta_{\tau\mu})=0.57$ in black one and $\cos(\theta_{\tau\mu})=0.17$ in green one.

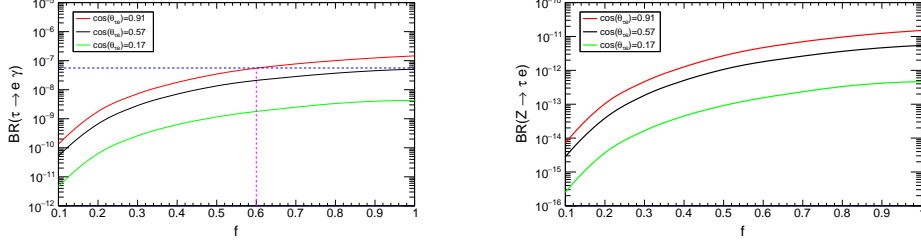


Fig. 8: $\text{BR}(\tau \rightarrow e\gamma)$ versus f (left), $\text{BR}(Z \rightarrow \tau e)$ versus f (right). For these two plots we set $\cos(\theta_{\tau e})=0.91$ in red line, $\cos(\theta_{\tau e})=0.57$ in black one and $\cos(\theta_{\tau e})=0.17$ in green one.

In Fig.8, we plot $\text{BR}(\tau \rightarrow e\gamma)$ versus the f parameter and $\text{BR}(Z \rightarrow \tau e)$ versus f at $\cos(\theta_{\tau e}) = 0.91, 0.57$ and 0.17 . The horizontal dotted blue line represents the current experimental limit of $\text{BR}(\tau \rightarrow e\gamma)$ as shown in table 7. It is clear that both $\text{BR}(\tau \rightarrow e\gamma)$ and $\text{BR}(Z \rightarrow \tau e)$ increase as the f parameter varies from 0.1 to 1. The prediction of $\text{BR}(\tau \rightarrow e\gamma)$ exceeds the current experimental limit at $f=0.6, 1, 1$ in red line, black and green one respectively. So, in this case the $\text{BR}(Z \rightarrow \tau e)$ is 4.61×10^{-12} , 5.5×10^{-12} and 4.65×10^{-13} at $f=0.60$ ($\cos(\theta_{\tau e})=0.91$), 1 ($\cos(\theta_{\tau e})=0.57$) and 1 ($\cos(\theta_{\tau e})=0.17$) respectively. Thus, under the constraints of $\tau \rightarrow e\gamma$ decay, the best predicted value of $\text{BR}(Z \rightarrow \tau e)$ is approximately 5×10^{-12} . The predicted value

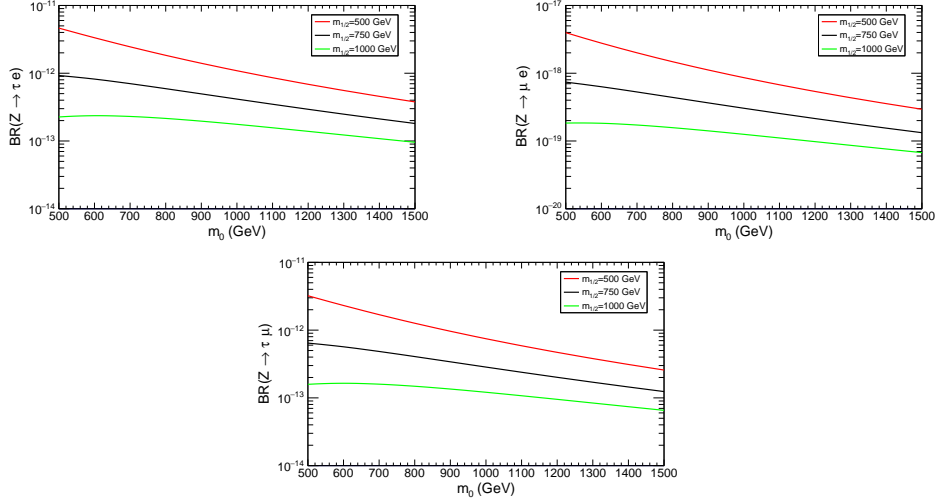


Fig. 9: $\text{BR}(Z \rightarrow l_i l_j)$ as a function of m_0 at $m_{1/2}=500, 750$ and 1000 GeV. For these two plots we set $\cos\theta_{ij}=0.91$ at $f=0.532$ for $\text{BR}(Z \rightarrow \tau e)$, $f=0.60$ for $\text{BR}(Z \rightarrow \tau e)$ and $f=0.015$ for $\text{BR}(Z \rightarrow \mu e)$.

is six orders of magnitude below the current experimental limit and four orders of

magnitude below the future experiments sensitivity as shown in table 1.

The two parameters, m_0 and $m_{1/2}$, are associated with the soft breaking slepton mass matrices and the soft breaking gaugino masses at the GUT scale. These parameters contribute to the sparticle masses at low energy. The masses of sleptons, sneutrinos, neutralinos and charginos contribute to LFV by one-loop functions in the electroweak interaction basis. The m_0 parameter also contributes in the non-diagonal elements of slepton matrices so both m_0 and $m_{1/2}$ have an effect on the LFV. Variations of $\text{BR}(Z \rightarrow l_i l_j)$ as a function of m_0 at $m_{1/2}=500, 750$ and 1000 GeV are shown in Fig.9. In this case we set $\cos\theta_{ij}=0.91$ and $f=0.532$ for $\text{BR}(Z \rightarrow \tau\mu)$, $f=0.60$ for $\text{BR}(Z \rightarrow \tau e)$ and $f=0.015$ for $\text{BR}(Z \rightarrow \mu e)$. The numerical results indicate that when $m_{1/2}$ increases, the branching ratios of Z decays decrease. When m_0 also increases from 500 to 1500 GeV, the BRs of Z decays have a small decrease. This indicates that large values of $m_{1/2}$ suppress the LFV in Z boson decays. Furthermore, under constraints on the $l_i \rightarrow l_j \gamma$ decays, the numerical results show that $\text{BR}(Z \rightarrow \mu e)$ is in the range $[6.7 \times 10^{-20}, 4 \times 10^{-18}]$, while $\text{BR}(Z \rightarrow \tau e)$ is in the range $[9.5 \times 10^{-14}, 4.6 \times 10^{-12}]$ and $\text{BR}(Z \rightarrow \tau\mu)$ is in the range $[6.5 \times 10^{-14}, 3.2 \times 10^{-12}]$.

5 Conclusions

The lepton flavor violation (LFV) of the Z boson decays ($Z \rightarrow l_i l_j$) in the constrained MSSM-Seesaw type-III model is studied in this article. In the supersymmetric models, the type-III seesaw mechanism can be realized by adding a fermionic triplet superfield. After deriving the analytical expressions for the branching ratios (BRs) of both Z boson and the radiative two body ($l_i \rightarrow l_j \gamma$) decays, we have studied numerically how BRs of the Z boson LFV decays can be predicted in this model. The numerical study has been performed by applying the following constraints: fitting to small neutrino masses, conserving the R-parity and the lightest SUSY particle of the considered model is the neutralino. Furthermore, the sparticle masses (charginos, sleptons, sneutrinos and neutralinos) should be above the recent experimental mass limits. We also applied constraints on the $\text{Br}(l_i \rightarrow l_j \gamma)$ and imposed the perturbativity limits on the parameters of this model. In order to investigate the small masses of the left-handed neutrinos, the mass of a fermionic triplet M_W should be in the order of 2.5×10^{13} GeV. After satisfying all constraints on the model parameters with (without) constraints on the $l_i \rightarrow l_j \gamma$ decays, the BRs maximum values of the Z boson LFV decays are summarized as in table 8.

Table 8: Values of the upper limits of the BRs of the Z boson LFV decays for this study, the ATLAS experiment and the future colliders (FCC-ee/CEPC). The statements Our results1(Our results2) means without(with) constraints on the $l_i \rightarrow l_j \gamma$ decays.

Z Decays	Our results ¹	Our results ²	LHC(90%)	FCC-ee/CEPC
$\text{BR}(Z \rightarrow \tau\mu)$	1.30×10^{-9}	$\sim 4.00 \times 10^{-12}$	7.20×10^{-6}	10^{-9}
$\text{BR}(Z \rightarrow \tau e)$	1.30×10^{-9}	$\sim 5.00 \times 10^{-12}$	7.00×10^{-6}	10^{-9}
$\text{BR}(Z \rightarrow \mu e)$	6.40×10^{-10}	$\sim 4.00 \times 10^{-18}$	2.62×10^{-7}	$10^{-8} - 10^{-10}$

These values are out of the experimental upper limits for the LHC, while they are in consistent with the sensitivity of the future colliders (FCC-ee/CEPC) for the scenario without constraints on the radiative two body decays ($l_i \rightarrow l_j \gamma$) as shown in table 8. However, after applying constraints on the $l_i \rightarrow l_j \gamma$ decays, the above-mentioned results get an additional suppression of about 10^{-3} for $\text{BR}(Z \rightarrow \tau l)$ and 10^{-8} for $\text{BR}(Z \rightarrow \mu e)$ when they are compered to the sensitivity of the future colliders (FCC-ee/CEPC). Hence, the BRs predictions are several orders below the recent experimental limits for both scenarios, which give a low probability to observe the Z boson LFV decays in the future collider experiments.

Acknowledgements. The authors would like to thank the administration of scientific research at Erzincan Binali Yildirim University/Türkiye, Al-Furat and Idlib University/Syria for supporting and funding this work.

A Appendix A: Vertexes

A.1 Two Fermions - Z Boson Interactions:

$$\Gamma_{i,j}^{\tilde{\chi}^0 \tilde{\chi}^0 Z, L} = -\frac{i}{2} \left(g_1 \sin \Theta_W + g_2 \cos \Theta_W \right) \left(N_{j3}^* N_{i3} - N_{j4}^* N_{i4} \right) \left(\gamma_\mu \cdot \frac{1 - \gamma_5}{2} \right) \quad (56)$$

$$\Gamma_{i,j}^{\tilde{\chi}^0 \tilde{\chi}^0 Z, R} = +\frac{i}{2} \left(g_1 \sin \Theta_W + g_2 \cos \Theta_W \right) \left(N_{i3}^* N_{j3} - N_{i4}^* N_{j4} \right) \left(\gamma_\mu \cdot \frac{1 + \gamma_5}{2} \right) \quad (57)$$

$$\Gamma_{i,j}^{\tilde{\chi}^+ \tilde{\chi}^- Z, L} = \frac{i}{2} \left(2g_2 U_{j1}^* \cos \Theta_W U_{i1} + U_{j2}^* \left(-g_1 \sin \Theta_W + g_2 \cos \Theta_W \right) U_{i2} \right) \left(\gamma_\mu \cdot \frac{1 - \gamma_5}{2} \right) \quad (58)$$

$$\Gamma_{i,j}^{\tilde{\chi}^+ \tilde{\chi}^- Z, R} = \frac{i}{2} \left(2g_2 V_{i1}^* \cos \Theta_W V_{j1} + V_{i2}^* \left(-g_1 \sin \Theta_W + g_2 \cos \Theta_W \right) V_{j2} \right) \left(\gamma_\mu \cdot \frac{1 + \gamma_5}{2} \right) \quad (59)$$

$$\Gamma_{i,j}^{\tilde{l} Z, L} = \frac{i}{2} \delta_{ij} \left(-g_1 \sin \Theta_W + g_2 \cos \Theta_W \right) \left(\gamma_\mu \cdot \frac{1 - \gamma_5}{2} \right) \quad (60)$$

$$\Gamma_{i,j}^{\tilde{l} Z, R} = -i g_1 \delta_{ij} \sin \Theta_W \left(\gamma_\mu \cdot \frac{1 + \gamma_5}{2} \right) \quad (61)$$

A.2 Two Scalars - Z Boson Interactions:

$$\Gamma_{i,j}^{\nu^I \nu^R Z} = \frac{1}{2} \left(g_1 \sin \Theta_W + g_2 \cos \Theta_W \right) \sum_{a=1}^3 Z_{ia}^{I,*} Z_{ja}^{R,*} \left(-p_\mu^{\nu_j^R} + p_\mu^{\nu_i^I} \right) \quad (62)$$

$$\Gamma_{i,j}^{\tilde{l}^* Z} = \frac{i}{2} \left(-2g_1 \sin \Theta_W \sum_{a=1}^3 Z_{i3+a}^{E,*} Z_{j3+a}^E + \right.$$

$$\left(-g_1 \sin \Theta_W + g_2 \cos \Theta_W\right) \sum_{a=1}^3 Z_{ia}^{E,*} Z_{ja}^E \left(-p_{\mu}^{\tilde{l}_j^*} + p_{\mu}^{\tilde{l}_i}\right) \quad (63)$$

A.3 Two Fermions - One Scalar Interactions:

$$\begin{aligned} \Gamma_{i,j,k}^{\tilde{\chi}^0 \tilde{l}^*, L} = & i \left(\frac{1}{\sqrt{2}} g_1 N_{i1}^* \sum_{a=1}^3 U_{L,ja}^{l,*} Z_{ka}^E + \frac{1}{\sqrt{2}} g_2 N_{i2}^* \sum_{a=1}^3 U_{L,ja}^{l,*} Z_{ka}^E \right. \\ & \left. - N_{i3}^* \sum_{b=1}^3 U_{L,jb}^{l,*} \sum_{a=1}^3 Y_{l,ab} Z_{k3+a}^E \right) \left(\frac{1-\gamma_5}{2} \right) \end{aligned} \quad (64)$$

$$\Gamma_{i,j,k}^{\tilde{\chi}^0 \tilde{l}^*, R} = + i \left(-\sqrt{2} g_1 \sum_{a=1}^3 Z_{k3+a}^E U_{R,ja}^l N_{i1} - \sum_{b=1}^3 \sum_{a=1}^3 Y_{l,ab}^* U_{R,ja}^l Z_{kb}^E N_{i3} \right) \left(\frac{1+\gamma_5}{2} \right) \quad (65)$$

$$\Gamma_{j,i,k}^{\tilde{\chi}^0 \tilde{e}, L} = i \left(-N_{j3}^* \sum_{b=1}^3 Z_{kb}^{E,*} \sum_{a=1}^3 U_{R,ia}^{l,*} Y_{l,ab} - \sqrt{2} g_1 N_{j1}^* \sum_{a=1}^3 Z_{k3+a}^{E,*} U_{R,ia}^{l,*} \right) \left(\frac{1-\gamma_5}{2} \right) \quad (66)$$

$$\Gamma_{j,i,k}^{\tilde{\chi}^0 \tilde{e}, R} = + i \left(\frac{1}{\sqrt{2}} \sum_{a=1}^3 Z_{ka}^{E,*} U_{L,ia}^l \left(g_1 N_{j1} + g_2 N_{j2} \right) - \sum_{b=1}^3 \sum_{a=1}^3 Y_{l,ab}^* Z_{k3+a}^{E,*} U_{L,ib}^l N_{j3} \right) \left(\frac{1+\gamma_5}{2} \right) \quad (67)$$

$$\Gamma_{i,j,k}^{\tilde{\chi}^- \nu^l, L} = -\frac{1}{\sqrt{2}} U_{j2}^* \sum_{b=1}^3 Z_{kb}^{I,*} \sum_{a=1}^3 U_{R,ia}^{l,*} Y_{l,ab} \left(\frac{1-\gamma_5}{2} \right) \quad (68)$$

$$\begin{aligned} \Gamma_{i,j,k}^{\tilde{\chi}^- \nu^l, R} = & + \frac{1}{4} \left(2\sqrt{2} g_2 \sum_{a=1}^3 Z_{ka}^{I,*} U_{L,ia}^l V_{j1} \right. \\ & \left. + v_u \left(\sum_{b=1}^3 Z_{kb}^{I,*} \sum_{a=1}^3 \kappa_{\nu,ab}^* U_{L,ia}^l + \sum_{b=1}^3 \sum_{a=1}^3 \kappa_{\nu,ab}^* Z_{ka}^{I,*} U_{L,ib}^l \right) V_{j2} \right) \left(\frac{1+\gamma_5}{2} \right) \end{aligned} \quad (69)$$

$$\Gamma_{i,j,k}^{\tilde{\chi}^- \nu^R, L} = i \frac{1}{\sqrt{2}} U_{j2}^* \sum_{b=1}^3 Z_{kb}^{R,*} \sum_{a=1}^3 U_{R,ia}^{l,*} Y_{l,ab} \left(\frac{1-\gamma_5}{2} \right) \quad (70)$$

$$\Gamma_{i,j,k}^{\tilde{\chi}^- \nu^R, R} = + \frac{i}{4} \left(-2\sqrt{2} g_2 \sum_{a=1}^3 Z_{ka}^{R,*} U_{L,ia}^l V_{j1} \right)$$

$$+ v_u \left(\sum_{b=1}^3 Z_{kb}^{R,*} \sum_{a=1}^3 \kappa_{\nu,ab}^* U_{L,ia}^l + \sum_{b=1}^3 \sum_{a=1}^3 \kappa_{\nu,ab}^* Z_{ka}^{R,*} U_{L,ib}^l \right) V_{j2} \left(\frac{1+\gamma_5}{2} \right) \quad (71)$$

$$\begin{aligned} \Gamma_{i,j,k}^{\tilde{\chi}^+ l \nu^I, L} &= \frac{1}{4} \left(-2\sqrt{2} g_2 V_{i1}^* \sum_{a=1}^3 U_{L,ja}^{l,*} Z_{ka}^{I,*} \right. \\ &\quad \left. - v_u V_{i2}^* \left(\sum_{b=1}^3 Z_{kb}^{I,*} \sum_{a=1}^3 U_{L,ja}^{l,*} \kappa_{\nu,ab} + \sum_{b=1}^3 U_{L,jb}^{l,*} \sum_{a=1}^3 Z_{ka}^{I,*} \kappa_{\nu,ab} \right) \right) \left(\frac{1-\gamma_5}{2} \right) \end{aligned} \quad (72)$$

$$\Gamma_{i,j,k}^{\tilde{\chi}^+ l \nu^I, R} = + \frac{1}{\sqrt{2}} \sum_{b=1}^3 Z_{kb}^{I,*} \sum_{a=1}^3 Y_{l,ab}^* U_{R,ja}^l U_{i2} \left(\frac{1+\gamma_5}{2} \right) \quad (73)$$

$$\begin{aligned} \Gamma_{i,j,k}^{\tilde{\chi}^+ e \nu^R, L} &= \frac{i}{4} \left(-2\sqrt{2} g_2 V_{i1}^* \sum_{a=1}^3 U_{L,ja}^{l,*} Z_{ka}^{R,*} + v_u V_{i2}^* \left(\sum_{b=1}^3 Z_{kb}^{R,*} \sum_{a=1}^3 U_{L,ja}^{l,*} \kappa_{\nu,ab} \right. \right. \\ &\quad \left. \left. + \sum_{b=1}^3 U_{L,jb}^{l,*} \sum_{a=1}^3 Z_{ka}^{R,*} \kappa_{\nu,ab} \right) \right) \left(\frac{1-\gamma_5}{2} \right) \end{aligned} \quad (74)$$

$$\Gamma_{i,j,k}^{\tilde{\chi}^+ l \nu^R, R} = + i \frac{1}{\sqrt{2}} \sum_{b=1}^3 Z_{kb}^{R,*} \sum_{a=1}^3 Y_{l,ab}^* U_{R,ja}^l U_{i2} \left(\frac{1+\gamma_5}{2} \right) \quad (75)$$

A.4 Two Scalars - γ Interactions:

$$\frac{i}{2} \left(2g_1 \cos \Theta_W \sum_{a=1}^3 Z_{i3+a}^{E,*} Z_{j3+a}^E + \left(g_1 \cos \Theta_W + g_2 \sin \Theta_W \right) \sum_{a=1}^3 Z_{ia}^{E,*} Z_{ja}^E \right) \left(-p_\mu^{\tilde{e}_j^*} + p_\mu^{\tilde{e}_i} \right) \quad (76)$$

A.5 Two Fermions - γ Interactions:

$$\frac{i}{2} \left(2g_2 U_{j1}^* \sin \Theta_W U_{i1} + U_{j2}^* \left(g_1 \cos \Theta_W + g_2 \sin \Theta_W \right) U_{i2} \right) \left(\gamma_\mu \cdot \frac{1-\gamma_5}{2} \right) \quad (77)$$

$$+ \frac{i}{2} \left(2g_2 V_{i1}^* \sin \Theta_W V_{j1} + V_{i2}^* \left(g_1 \cos \Theta_W + g_2 \sin \Theta_W \right) V_{j2} \right) \left(\gamma_\mu \cdot \frac{1+\gamma_5}{2} \right) \quad (78)$$

References

- [1] Esteves, J.N., Hirsch, M., Porod, W., Romao, J.C., Valle, J.W.F., Moral, A. J. High Energ. Phys. **2009** (2009) <https://doi.org/10.1088/1126-6708/2009/05/003> [arXiv:0903.1408](https://arxiv.org/abs/0903.1408) [hep-ph]

- [2] Primulandoando, R., Julio, J., Uttayarat, P. , J. High Energ. Phys. **02** (2022) [https://doi.org/10.1007/JHEP08\(2019\)024](https://doi.org/10.1007/JHEP08(2019)024) arXiv:1903.02493 [hep-ph]
- [3] Fukuda, Y., Hayakawa, T., Ichihara, E., Inoue, K., Ishihara, K., Ishino, H., Itow, Y., Kajita, T. , Phys. Rev. Lett. **81**, 1562–1567 (1998) <https://doi.org/10.1103/PhysRevLett.81.1562>
- [4] Ahmad, Q.R., Allen, R.C., Andersen, T.C., D.Anglin, J., Barton, J.C. , Phys. Rev. Lett. **89**, 011301 (2002) <https://doi.org/10.1103/PhysRevLett.89.011301> arXiv:nucl-ex/0204008 [hep-ph]
- [5] Eguchi, K., Enomoto, S., Furuno, K., Goldman, J., Hanada, H., Ikeda, H., Ikeda, K., Inoue, K. , Phys. Rev. Lett. **90**, 021802 (2003) <https://doi.org/10.1103/PhysRevLett.90.021802> arXiv:hep-ex/0212021 [hep-ph]
- [6] Abe, S., Ebihara, T., Enomoto, S., Furuno, K., Gando, Y., Ichimura, K. , Phys. Rev. Lett. **100**, 221803 (2008) <https://doi.org/10.1103/PhysRevLett.100.221803> arXiv:0801.4589 [hep-ph]
- [7] KATRIN collaboration , Phys. Rev. D **104**, 012005 (2021) <https://doi.org/10.1103/PhysRevD.104.012005> arXiv:2101.05253 [hep-ph]
- [8] KATRIN collaboration , Nature Physics **18**, 160–166 (2022) <https://doi.org/10.1038/s41567-021-01463-1> arXiv:2105.08533 [hep-ph]
- [9] Han, C., Lei, Z., Liao, W. Chinese Physics C **47**(9), 093104 (2023) <https://doi.org/10.1088/1674-1137/ace708> arXiv:2303.15709 [hep-ph]
- [10] Li, Z., Wang, F. , Eur. Phys. J. C **80** (2020) <https://doi.org/10.1140/epjc/s10052-020-8373-0> arXiv:2001.04155 [hep-ph]
- [11] Hirsch, M., Joaquim, F.R., Vicente, A. , J. High Energ. Phys. **2012** (2012) [https://doi.org/10.1007/JHEP11\(2012\)105](https://doi.org/10.1007/JHEP11(2012)105) arXiv:1207.6635 [hep-ph]
- [12] Minkowski, P. Physics Letters B **67**(4), 421–428 (1977) [https://doi.org/10.1016/0370-2693\(77\)90435-X](https://doi.org/10.1016/0370-2693(77)90435-X)
- [13] Yanagida, T. , KEK Report No. 79-18 **95** (1979)
- [14] Gell-Mann, M., Ramond, P., Slansky, R., Van Nieuwenhuizen, P., Freedman, D. , North-Holland Amsterdam (1979)
- [15] Mohapatra, R.N., Senjanović, G. , Phys. Rev. Lett. **44**, 912–915 (1980) <https://doi.org/10.1103/PhysRevLett.44.912>
- [16] Schechter, J., Valle, J.W.F. , Phys. Rev. D **22**, 2227–2235 (1980) <https://doi.org/10.1103/PhysRevD.22.2227>

- [17] Foot, R., Lew, H., He, X.-G., Joshi, G.C. , Zeitschrift für Physik C Particles and Fields **44**, 441–444 (1989) <https://doi.org/10.1007/BF01415558>
- [18] Ma, E. , Phys. Rev. Lett. **81**, 1171–1174 (1998) <https://doi.org/10.1103/PhysRevLett.81.1171>
- [19] Schechter, J., Valle, J.W.F. , Phys. Rev. D **25**, 774–783 (1982) <https://doi.org/10.1103/PhysRevD.25.774>
- [20] Konetschny, W., Kummer, W. , Physics Letters B **70**(4), 433–435 (1977) [https://doi.org/10.1016/0370-2693\(77\)90407-5](https://doi.org/10.1016/0370-2693(77)90407-5)
- [21] Marshak, R.E., Mohapatra, R.N., pp. 277–287. Springer, Boston, MA (1980). https://doi.org/10.1007/978-1-4613-3165-0_18 . https://doi.org/10.1007/978-1-4613-3165-0_18
- [22] Cheng, T.P., Li, L.-F. , Phys. Rev. D **22**, 2860–2868 (1980) <https://doi.org/10.1103/PhysRevD.22.2860>
- [23] Lazarides, G., Shafi, Q., Wetterich, C. , Nuclear Physics B **181**(2), 287–300 (1981) [https://doi.org/10.1016/0550-3213\(81\)90354-0](https://doi.org/10.1016/0550-3213(81)90354-0)
- [24] Mohapatra, R.N., Senjanović, G. , Phys. Rev. D **23**, 165–180 (1981) <https://doi.org/10.1103/PhysRevD.23.165>
- [25] Sun, K.-S., Chen, J.-B., Yang, X.-Y., Cui, S.-K. , Chinese Physics C **43**(4), 043101 (2019) <https://doi.org/10.1088/1674-1137/43/4/043101> arXiv:1901.03800 [hep-ph]
- [26] Jurčiukonis, D., Lavoura, L. , J. High Energ. Phys. **2022** (2022) [https://doi.org/10.1007/JHEP03\(2022\)106](https://doi.org/10.1007/JHEP03(2022)106) arXiv:2107.14207 [hep-ph]
- [27] Sun, K.-S., Zhang, W.-H., Chen, J.-B., Zhang, H.-B., Yan, Q.-g. Chinese Physics C **47**(7), 073106 (2023) <https://doi.org/10.1088/1674-1137/acd3da> arXiv:2204.06234 [hep-ph]
- [28] Abada, A., Figueiredo, A.J.R., Romão, J.C., Teixeira, A.M. , J. High Energ. Phys. **2011** (2011) [https://doi.org/10.1007/JHEP08\(2011\)099](https://doi.org/10.1007/JHEP08(2011)099) arXiv:1104.3962 [hep-ph]
- [29] Altmannshofer, W., Caillol, C., Dam, M., Xella, S., Zhang, Y.: (2022). <https://arxiv.org/abs/2205.10576>
- [30] ATLAS collaboration , Phys. Rev. Lett. **127**, 271801 (2021) <https://doi.org/10.1103/PhysRevLett.127.271801> arXiv:2105.12491 [hep-ph]
- [31] ATLAS collaboration , Phys. Rev. D **108**, 032015 (2023) <https://doi.org/10.1103/PhysRevD.108.032015> arXiv:2204.10783 [hep-ph]

- [32] Hundi, R.S. , Eur. Phys. J. C **82505** (2022) <https://doi.org/10.1140/epjc/s10052-022-10453-3> arXiv:2201.03779 [hep-ph]
- [33] Calibbi, L., Marcano, X., Roy, J. , Eur. Phys. J. C **81**, 1054 (2021) <https://doi.org/10.1140/epjc/s10052-021-09777-3> arXiv:2107.10273 [hep-ph]
- [34] Cao, J., Xiong, Z., Yang, J.M. ,The European Physical Journal C **32**, 245–252 (2004) <https://doi.org/10.1140/epjc/s2003-01391-1> arXiv:hep-ph/0307126 [hep-ph]
- [35] Illana, J.I., Masip, M. Phys. Rev. D **67**, 035004 (2003) <https://doi.org/10.1103/PhysRevD.67.035004> arXiv:hep-ph/0207328 [hep-ph]
- [36] Dong, X.-X., Zhao, S.-M., Zhan, X.-J., Yang, Z.-J., Zhang, H.-B., Feng, T.-F. , Chinese Physics C **41**(7), 073103 (2017) <https://doi.org/10.1088/1674-1137/41/7/073103> arXiv:1704.02202 [hep-ph]
- [37] Esteves, J.N., Romao, J.C., Hirsch, M., Staub, F., Porod, W. , Phys. Rev. D **83**, 013003 (2011) <https://doi.org/10.1103/PhysRevD.83.013003> arXiv:1010.6000 [hep-ph]
- [38] Buckley, M.R., Murayama, H. Phys. Rev. Lett. **97**, 231801 (2006) <https://doi.org/10.1103/PhysRevLett.97.231801> arXiv:hep-ph/0606088 [hep-ph]
- [39] Hirsch, M., Porod, W., Weiss, C., Staub, F. , Phys. Rev. D **87**, 013010 (2013) <https://doi.org/10.1103/PhysRevD.87.013010> arXiv:arXiv:1211.0289 [hep-ph]
- [40] Hirsch, M., Reichert, L., Porod, W. J. High Energ. Phys. **2011** (2011) [https://doi.org/10.1007/JHEP05\(2011\)086](https://doi.org/10.1007/JHEP05(2011)086) arXiv:1101.2140 [hep-ph]
- [41] Basso, L., Belyaev, A., Chowdhury, D., Hirsch, M., Khalil, S., Moretti, S., O’Leary, B., Porod, W., Staub, F. , Computer Physics Communications **184**(3), 698–719 (2013) <https://doi.org/10.1016/j.cpc.2012.11.004> arXiv:1206.4563 [hep-ph]
- [42] CSÁKI, C. ,Modern Physics Letters A **11**(08), 599–613 (1996) <https://doi.org/10.1142/S021773239600062X> arXiv:9606414 [hep-ph]
- [43] Rossi, A. , Phys. Rev. D **66**, 075003 (2002) <https://doi.org/10.1103/PhysRevD.66.075003> arXiv:hep-ph/0207006 [hep-ph]
- [44] Yang, J. ,Science China Physics, Mechanics and Astronomy **53**, 1949–1952 (2010) <https://doi.org/10.1007/s11433-010-4146-3> arXiv:1006.2594 [hep-ph]
- [45] De Romeri, V., Herrero, M.J., Marcano, X., Scarcella, F. , Phys. Rev. D **95**, 075028 (2017) <https://doi.org/10.1103/PhysRevD.95.075028> arXiv:1607.05257 [hep-ph]

- [46] Marcano, X., p. 162. Springer (2018). <https://doi.org/10.1007/978-3-319-94604-7>
- [47] Porod, W., Staub, F., Vicente, A. , Eur. Phys. J. C **74** (2014) <https://doi.org/10.1140/epjc/s10052-014-2992-2> arXiv:1405.1434 [hep-ph]
- [48] Bi, X.-J., Dei, Y.-B., Qi, X.-Y. , Phys. Rev. D **63**, 096008 (2001) <https://doi.org/10.1103/PhysRevD.63.096008>
- [49] Passarino, G., Veltman, M. ,Nuclear Physics B **160**(1), 151–207 (1979) [https://doi.org/10.1016/0550-3213\(79\)90234-7](https://doi.org/10.1016/0550-3213(79)90234-7)
- [50] Hahn, T. ,Nuclear Physics B - Proceedings Supplements **89**(1), 231–236 (2000) [https://doi.org/10.1016/S0920-5632\(00\)00848-3](https://doi.org/10.1016/S0920-5632(00)00848-3) arXiv:hep-ph/0005029. Loops and Legs in Quantum Field Theory
- [51] Patel, H.H. ,Computer Physics Communications **197**, 276–290 (2015) <https://doi.org/10.1016/j.cpc.2015.08.017> arXiv:1503.01469 [hep-ph]
- [52] Staub, F. , Computer.Physics.Commun. **181**, 1077–1086 (2010) <https://doi.org/10.1016/j.cpc.2010.01.011> arXiv:0909.2863 [hep-ph]
- [53] Staub, F. , Computer.Physics.Commun. **185**, 1773–1790 (2014) <https://doi.org/10.1016/j.cpc.2014.02.018> arXiv:1309.7223 [hep-ph]
- [54] Goodsell, M.D., Nickel, K., Staub, F. , Eur. Phys. J. C **75** (2015) <https://doi.org/10.1140/epjc/s10052-014-3247-y> arXiv:1411.0675 [hep-ph]
- [55] Bernigaud, J., Forster, A.K., Herrmann, B., King, S.F., Porod, W., Rowley, S.J. , J. High Energ. Phys. **2022** (2022) [https://doi.org/10.1007/JHEP05\(2022\)156](https://doi.org/10.1007/JHEP05(2022)156) arXiv:2111.10199 [hep-ph]
- [56] Navas, S., (Particle Data Group) , Phys. Rev. D **110**, 030001 (2024) <https://doi.org/10.1103/PhysRevD.110.030001>
- [57] Hirsch, M., Kaneko, S., Porod, W. , Phys. Rev. D **78**, 093004 (2008) <https://doi.org/10.1103/PhysRevD.78.093004> arXiv:0806.3361 [hep-ph]
- [58] BELLE collaboration , J. High Energ. Phys. **2021** (2021) [https://doi.org/10.1007/JHEP10\(2021\)019](https://doi.org/10.1007/JHEP10(2021)019) arXiv:2103.12994 [hep-ph]
- [59] MEG collaboration , Eur. Phys. J. C **76** (2016) <https://doi.org/10.1140/epjc/s10052-016-4271-x> arXiv:1605.05081 [hep-ph]
- [60] Hisano, J., Moroi, T., Tobe, K., Yamaguchi, M. , Phys. Rev. D **53**, 2442–2459 (1996) <https://doi.org/10.1103/PhysRevD.53.2442> arXiv:hep-ph/9510309 [hep-ph]